Toward High Resolution Evapotranspiration Estimation for Drought Impacts on Crops

Evaluation of evapotranspiration heterogeneity over the Netherlands

Saeid Asadollahi Dolatabad
Enschede,The Netherlands, February, 2015

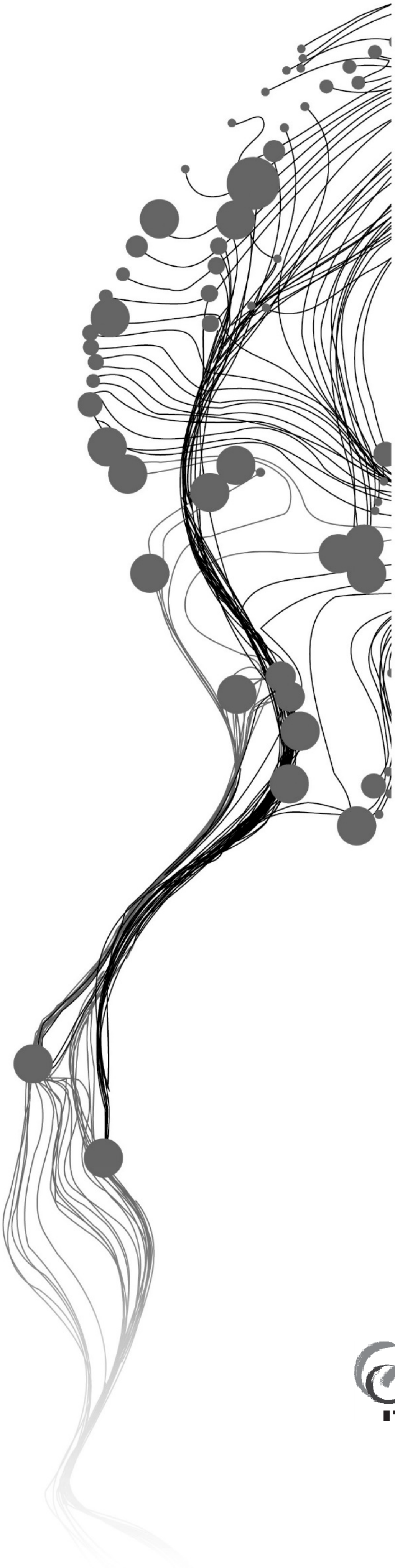

Toward High Resolution Evapotranspiration Estimation for Drought Impacts on Crops

Evaluation of evapotranspiration heterogeneity over the Netherlands

Saeid Asadollahi Dolatabad
Enschede,The Netherlands, February, 2015

Thesis submitted to the Faculty of Geo-Information Science and Earth Observation of the University of Twente in partial fulfilment of the requirements for the degree of Master of Science in Geo-information Science and Earth Observation.
Specialization: Water Resources and Environment Management

THESIS ASSESSMENT BOARD:
Prof. Dr. Ir. Z. Su (Chair)]
Dr. ir. C.A.J.M. de Bie (External Examiner, University of Twente)
Dr. Ir. J. Timmermans
Dr. B.H.P. Maathuis

Department of Water Resources
Faculty of Geo-Information Science and Earth Observation

ABSTRACT

Currently, the global needs for food and water is at a critical level. It has been estimated that 12.5 % of the global population suffers from malnutrition and 768 million people still do not have access to clean drinking water. This need is increasing because of the population growth and climate change. Changes in precipitation patterns will result either in flooding or droughts. Consequently availability, usability and affordability of water is becoming challenge and efficient use of water and water management is becoming more important, particularly during severe drought events.

Drought monitoring for agricultural purposes is very hard. While meteorological drought can accurately be monitored using precipitation only, estimating agricultural drought is more difficult. This is because agricultural drought is dependent on the meteorological drought, the impacts on the vegetation, and the resilience of the crops. As such not only precipitation estimates are required but also evapotranspiration at plant/plot scale is needed.

Evapotranspiration (ET) describes the amount of water evaporated from soil and vegetation. As 65% of precipitation is lost by ET, drought severity is highly linked with this variable. In drought research, the precise quantification of ET and its spatial-temporal variability is therefore essential. In this view, remote sensing based models to estimate ET, such as SEBAL and SEBS, are of high value.

However the resolution of current evapotranspiration products are not good enough for monitoring the impact of the droughts on the specific crops. This limitation originates because plot scales are in general smaller than the resolution of the available satellite ET products. As such while land surface heterogeneity affects ET, in coarse resolution remote sensing based ET estimations always a combination of different land surface types is taken to account and cannot be used for plant health and drought resilience studies. Consideration of crop characteristics in ET estimation is therefore improves the results in agricultural drought monitoring.

The goal of this research is using crop characteristic and land surface heterogeneity to enable adequate resolutions of daily evapotranspiration estimates for monitoring crop health during the severe drought events.

Keywords: Drought, ET, SEBS, MODIS, LANDSAT, NDVI, Crop coefficient, water stress ratio.

ACKNOWLEDGEMENTS

First of all thanks to God for helping me during the whole of my life.
I would like to express my gratitude to the The European Union's Erasmus Mundus program to provide me this opportunity to pursue Master of Science degree at Unversity of Twente - Faculty of Geo-information Science and Earth Observation.
I would like to thank my first supervisor, Dr. Ir. Joris Timmermans for his excellent guidance during the research period. He was so helpful for me for all the period of my thesis from the beginning to the end. I wish him success and prosperity.
I want to thank to my dear lovely wife for her helps, her kindliness and her love.
I am also thankful from my second supervisor Dr. Ben Maathuis for his guidance.
I would like to thank all the staff members of WRS department at ITC for enriching us with their valuable knowledge during the period of my study here at ITC.
My sincere thanks to my mother and my family for their love in my heart.

TABLE OF CONTENTS

Contents

LIST OF FIGURES

LIST OF TABLES

1. INTRODUCTION

1.1. Background:

The global need for water and food is critical. It has been estimated that 12.5 % of the global population suffers from malnutrition ("2013 World Hunger and Poverty Facts and Statistics by World Hunger Education Service," n.d.) and 768 million people still do not have access to clean drinking water("UNICEF Water and Sanitation," n.d.). This need is also increasing because of population growth and impact of climate change(FAO - Food and Agriculture Organization of the United Nations, n.d.). The change in precipitation patterns (caused by climate change) results in flooding in one part of the world and drought in the other. In addition global temperatures are getting higher due to the effect of climate change("Climate Change Effects," n.d.), so water demand for crop feeding will be growth in the future. Currently 10% of terrestrial surface are crop lands. Irrigated croplands that use 80% of human water consumption provide 45% of food supply of the world (M. Anderson & Kustas, 2008). The water consumption by all agriculture is estimated to be 6700 km3/year which is about 80 of the global water consumption. With the projected increases in droughts, a competition between food production and drinkable water resources will emerge. Consequently availability, usability and affordability of water is becoming challenge and efficient use of water and water management is becoming more important (M. Anderson & Kustas, 2008). Research into allocation water resources is therefore not only important in terms of drinking water, but also for agricultural demand.

1.1.1. Drought types

Drought is caused by the interaction between precipitation, evapotranspiration (ET) and water demand. It is different from other natural hazards because such events occurs slowly and with time delay. Drought detection is very hard and therefore causes severe impacts such as loss in agricultural production, reduction of water levels, famine and migration of people (Karavitis, Alexandris, Tsesmelis, & Athanasopoulos, 2011). Droughts therefore have been categorized in different categories on basis of their impacts: Meteorological, Agricultural and Hydrological (Wilhite and Glantz, 1985)

- Meteorological drought is defined as deficiency of rainfall or increment of evapotranspiration in a long time.
- Agricultural drought links various characteristics of meteorological drought to agricultural impacts. It focusses on the reduced availability of water to plants and consequently the reduction of food production("Types of Drought," n.d.).
- Hydrological drought occurs when supply of surface and subsurface water falls below the normal level.

1.1.2. Drought severity

Researches on drought should provide severity of the drought event, irrespective of 1) the event 2) the period and 3) the study area. Therefore such severities are described in objective indices which can be cross-compared against each other. Some of indices used for assessing severity of drought are described in Table 1-1 (Michael J. Hayes, Mark. D. Svoboda, Donald A. Wilhite, 1999).

Table 1-1. Different types of drought indices

Drought index	abbreviation	explanation
Standardized precipitation index	SPI	Calculated solely on precipitation. It is computed for different time scales: 3, 6, 12, 24, 48 months
Palmer drought severity index	PDSI	Calculated based on precipitation, temperature, soil moisture.
Crop moisture index	CMI	Calculated based on short term soil moisture condition, using weekly precipitation and mean temperature.in growing season
Surface water supply index	SWSI	Complement to PDSI. Calculated based on snowpack, stream flow, precipitation and reservoir storage.
Water Requirement Satisfaction Index	WRSI	It is based on ratio of actual ET of crop to reference ET crop
Evapotranspiration deficit index	ETDI	It is based on water stress ratio

1.1.3. Drought severity by Evapotranspiration

Evapotranspiration (ET) describes the amount of water evaporated from soil and vegetation. As 65% of precipitation is lost by ET, drought severity is highly linked with this variable (Eden, 2012). The precise quantification of ET and its spatial-temporal variability is therefore essential, in particular for the evaluation of agricultural droughts. Specific agricultural drought indices that used on evapotranspiration and water stress are:

- **Water Requirement Satisfaction Index (WRSI):** Based on the availability of water for crops during growing season. It is based on ratio of actual crop ET (ET_a) to crop water requirement that is calculated from reference crop ET (ET_{ref}) and crop coefficient.

$$WRSI = \frac{ET_a}{ET_{ref}} \qquad \text{Equation 1-1}$$

- **Water stress ratio ($\boldsymbol{WS}$)**: This WS is calculated on basis of the water stress anomaly (Equation 1-2) using water stress ratio that has value from 0 to1 by the equation. Value 1 means no ET and 0 means actual ET occurs at the range of reference ET. The difference between WS and WRSI is that water stress ratio considers seasonality, while in WRSI seasonality isn't taken to account.

$$WS = \frac{ET_{ref} - ET_a}{ET_{ref}}$$ Equation 1-2

- **Evapotranspiration deficit index (ETDI):** This is calculated based on WS and considers seasonal averages of this parameter as well. In this index weekly WS is calculated Equation 1-3 and Equation 1-4 and based on the minimum, maximum and average of that by using Equation 1-5 the index ETDI is calculated

$$WS_{A_{ij}} = \frac{MWS_j - WS_{ij}}{MWS_j - minWS_{ij}} * 100 \qquad \text{If } WS_{ij} \leq MWS_j$$ Equation 1-3

$$WS_{A_{ij}} = \frac{MWS_j - WS_{ij}}{\max WS_{ij} - MWS_j} * 100 \qquad \text{If } WS_{ij} > MWS_j$$ Equation 1-4

$$ETDI_j = 0.5\ ETDI_{j-1} + WS_{A_j}/50$$ Equation 1-5

The major difference between the WRSI and ETDI methods lies within the containing seasonal behaviour of ETDI, (which the WRSI does not take into account).

1.1.4. Evapotranspiration Estimation

There are many methods for estimating of evapotranspiration: either based on measurements on the ground or estimations from remote sensing. Ground based estimation is currently done via lysimeters, bowen ratio towers, scintillometers and eddy covariance measurements (Spiliotopoulos et al., 2013) (Yang, Zhang, Wang, & Zhou, 2014). In contrast, remote sensing provides the possibility of estimating ET at regular intervals for large scales. However, As ET cannot be directly measured from space, relevant physical parameters need to be observed (Su, 2002) and models are required for deriving ET from these parameters. Consequently remote sensing based models estimate ET indirectly on basis of relevant physical variables.
Some available methods for estimating ET by remote sensing are:

- SEBAL (Bastiaanssen, 1998)
- SEBS (Su, 2002)
- ALEXI/ DisALEXI (Norman,2003)

SEBS is recommended over other surface energy models because:

- It is physically based model, so applicable for different conditions. As "It has been applied widely for heterogeneous areas" (Liou & Kar, 2014).
- It minimizes uncertainty in surface temperature and meteorological variables (Eden, 2012).
- It has the potential to model ET over short or long time steps and over diverse sets of meteorological conditions (Glenn, Huete, Nagler, Hirschboeck, & Brown, 2007).

MODIS satellite data is used in SEBS algorithm because it contains land surface temperature (LST).

1.1.5. Drought in the Netherlands

Drought in the Netherlands has been marginalized for a long time. Local people do not consider the possibility of droughts in some part of the Europe. the Netherlands has suffered severe droughts in years 2003 and 2006 (Eden, 2012). Such events will become more frequent in the future due to climate change. In the Netherlands the Royal Dutch Meteorological Institute (KNMI) uses deficit method for measuring water deficit. This KNMI index is based on the difference between precipitation and potential evaporation. The start date is always 1st of April that is the first official day of the growing season and it ends at last day of September (Broek, Teuling, & Loon, 2014). In the Figure 1-1 graph shows in the year 1976 (the red line) and in year 2003 (the black line) this deficit was critical.

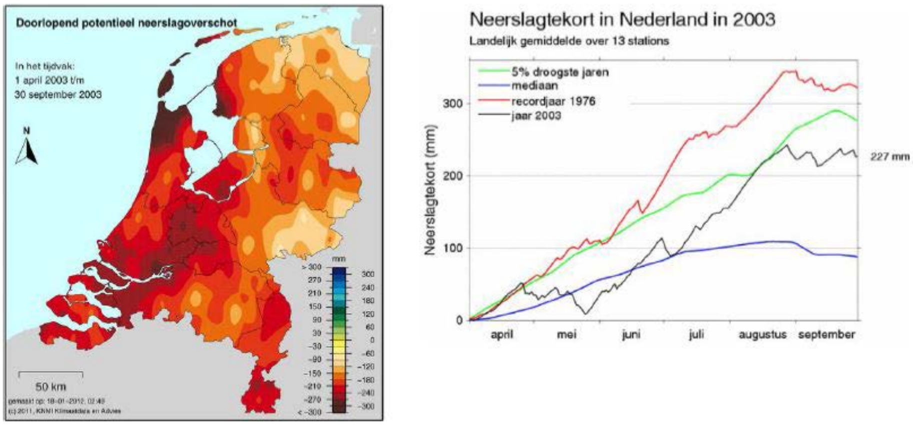

Figure 1-1. The interpolated drought map and a graph which shows the precipitation deficit in time (KNMI, 2014).

Table 1-2. Overview of the drought events in The Netherlands from 1950 to 2011 (KNMI, 2014) (Broek et al., 2014)

Period	Drought characteristics
1976	Drought year, especially during the growing season. Precipitation amount was 536 mm (833 mm is the long-term average of 1981-2010)
1995	During the months August and October. No drought during growing season.
1997	During the months January and March
2003	A significant dry year, belongs to the 5% of driest years
2006	During the growing season especially for months June and July
2007	During the months March, April and May
2011	During the months April and May

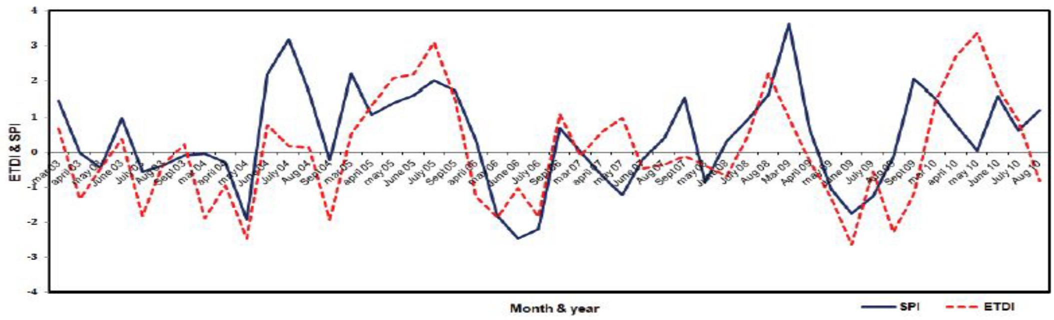

Figure 1-2. Yearly drought monitoring in the Twente region based on SPI and ETDI (Eden, 2012)

In addition as shown in Figure 1-3 (Eden, 2012) analysis on the temperature trend over the past years at two stations in Twente and de Bilt shows, there is positive deviation of temperature from the mean. This will lead to higher evaporative rates and therefore also lead to increasing frequencies of drought in the Netherlands. Consequently it is of high necessity to investigate droughts in the Netherlands and the impacts of it on food production (Eden, 2012).

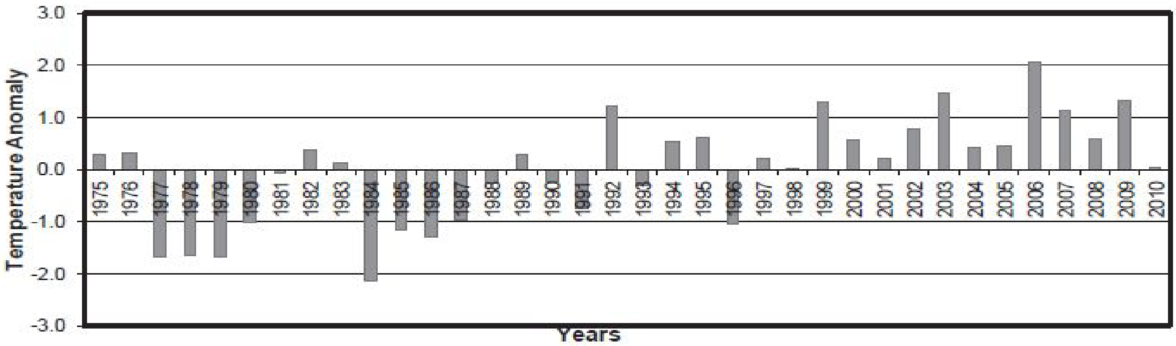

Figure 1-3. Temperature anomalies for Twente region (1975-2010) (Eden, 2012)

1.2. Problem Statement

The impact of Droughts in the Netherlands is currently marginalized. However there are clear indications that droughts have impacts on the crops as:

- Although some agricultural fields in the Netherlands use irrigation system, most of them are rain-fed, so in prolonged dry periods after intense rainfalls crops get damaged.
- Although because of precipitation the Netherlands has good supply of groundwater, Crops have small and short roots, so they cannot uptake water from ground water and prolonged dryness will harm them.
- In the Netherlands the growing season always starts from 1st of April and finishes around the 30th of September (Beersma & Buishand, 2007) In this period, the total amount of precipitation is less than the total evaporated amount of water. As such, the water cycle is highly vulnerable for droughts (Broek et al., 2014). There are several studies, indicate that severe drought events will grow more frequent. The impact of this increasing dryness periods on agriculture therefore needs to be investigated.
- However investigation impacts of drought on the crops in the Netherlands becomes difficult, because plot sizes in the Netherlands are small. As such spatial resolution of frequently overpassing satellites sensors is too low while frequencies of high resolution sensors is too low for drought monitoring (M. C. Anderson, Allen, Morse, & Kustas, 2012).

1.3. Research Objective

The aim of this research is assess the subpixel heterogeneity of coarse resolution evapotranspiration in order to monitoring impacts of drought on crops in the Netherlands.

1.3.1. Specific research objectives:

The main objective can be split into several specific research objectives:

1. Investigating impacts of known droughts on coarse resolution ET estimation in period 2002 till 2014.
2. Estimating crop coefficients on basis of high resolution NDVI.
3. Determining adequate monitoring characteristics (spatial and temporal resolution) for drought impact on crop growths.
4. Estimating the impact of subpixel heterogeneity on coarse resolution evapotranspiration by crop.
5. Disaggregation data of different satellites for deriving high spatial and temporal resolution images for ET estimation.
6. Monitoring behaviour of crops at plot scale, during 2003/2006 drought season

1.3.2. Research Questions

- How we can use land cover/land use map for upscaling coarse spatial resolution ET?
- How we can use the result of this research for monitoring effect of drought on crops?
- How we can use the result of this research for water management?

1.4. Outline of the thesis

The outline this thesis is as follows: After the background information, a literature review is performed which forms the basis of the research methodology. Afterwards the data processing is described. Finally the results and conclusions of this research are provided. The Data processing and results section have the same structure namely:

1st Coarse resolution ET estimation is evaluated with ground based data, 2nd the thesis describes the investigation of heterogeneity on ET.

- Reviewing different crop growth steps for each type of crop with remote sensing method.
- Providing high resolution Kc map for disaggregation of coarse resolution ET to high resolution.
- Using high resolution Kc map to investigate impact of agricultural drought on each type of crops with high resolution estimation.
- Obtaining water stress ratio for using in monitoring impact of agricultural drought on crops.

2. LITERATURE REVIEW

In this research concepts of evapotranspiration, drought, and disaggregation are regularly used. A lot of research has been performed on these specific important concepts. A short but comprehensive overview of these concepts and researches is provided below.

2.1. Evapotranspiration

Evapotranspiration (ET) describes the loss of water from earth surface to the atmosphere. Loss of water from water body or bare soil called evaporation and from vegetation or living surface called transpiration(Li et al., 2009). This combined loss of water is therefore an important factor in the water and energy cycle. Global average ET is more than 50% of average precipitation while in arid and semi-arid area this value will be more higher (Glenn & Brown, 2009). So it is as important as precipitation in characterizing the water cycle.

Three types of evapotranspiration are identified:

- Reference evapotranspiration
- Potential evapotranspiration
- Actual evapotranspiration

2.1.1. Reference evapotranspiration

Reference evapotranspiration (ET_{ref}) represents the potential ET for a reference crop under well watered conditions. The FAO Penman–Monteith equation is used commonly for reference evapotranspiration estimation. This is based on FAO-56 definition, where the reference crop is a grass with an assumed height of 0.12 m, with a surface resistance of 70 s/m and an albedo of 0.23 (Allen, 2000)(Gelassie, 2012). The FAO Penman- Monteith method to estimate ET_{ref} can be derived by Equation 2-1:

$$ET_{ref} = \frac{0.408\,\Delta\,(R_n - G) + \gamma\,\frac{900}{T+273}\,U_2\,(e_s - e_a)}{\Delta + \gamma(1 + 0.34\,U_2)} \qquad \text{Equation 2-1}$$

Where: ET_{ref} is reference evapotranspiration [mm day^{-1}], R_n is net radiation at the crop surface [MJ$m^{-2}day^{-1}$], G is soil heat flux [MJ$m^{-2}day^{-1}$], T is mean daily air temperature at 2m height[°C], U_2 is wind speed at 2 m height [ms^{-1}], e_s is saturation vapor pressure [kPa], e_a is actual vapor pressure [kPa], Δ is slope vapour pressure curve [kPa°C^{-1}] and γ is psychrometric constant.

2.1.2. Potential evapotranspiration

$$ET_p = ET_{ref} * K \quad \text{Equation 2-2}$$

$$K = \max(K_c, K_s) \quad \text{Equation 2-3}$$

ET_p represents potential evapotranspiration. Crop coefficient (K_c) is the ratio of crop ET to the reference evapotranspiration (ET_{ref}). It represents the characteristics that cause distinction between crop ET and ET_{ref}. These characteristics are crop height (affecting roughness and aerodynamic resistance), surface resistance (affected by leaf area, the fraction of ground covered by vegetation, leaf age and condition, and soil surface wetness) and albedo of the surface (affected by the fraction of ground covered by vegetation and by the soil surface wetness). ET estimation based on remote sensing approaches is the estimation for the time that satellite or airplane passes over the specific study region. For the time between the instances, ET predicting needs the application of ratio of ET/ET_{ref} or an evaporative fraction, EF (Bastiaanssen, 2000) Actual evapotranspiration

Actual evapotranspiration can be calculated from the potential evapotranspiration on basis of the water stress coefficient (FAO).

$$ET_a = ET_p * K_s \quad \text{Equation 2-4}$$

However information that concerns the water stress coefficient are difficult to obtain. The Actual evapotranspiration process depends greatly on the source of water, source of energy and a sink for vapor. Consequently other methods have been created for directly estimating actual evapotranspiration independent of the reference and potential evapotranspiration:

1) Mass budget methods;
2) Energy budget methods,
3) Methods based on measurements of mean profiles and atmospheric turbulence (Kalma, McVicar, & McCabe, 2008).

Traditional approaches of ET estimation done based on meteorological data by using Energy Balance Bowen ratio, eddy covariance techniques, pan-measurement, weighing lysimeter, scintillometer and sap flow, that are based on the field measurement methods. These methods are accurate at local scales. However, such measurements cannot fully characterize the evapotranspiration in heterogeneous areas or at large scales because of complexity of hydrologic processes (Kalma et al., 2008) (Gelassie, 2012).

Remote sensing based ET estimation therefore provides the solution for solving this problem because satellites provides regular observations with a large spatial coverage. In addition these observations costs less than the same spatial information that is obtained with field measurement (Kalma et al., 2008). Also it is so useful for the area that man-made measurement are so difficult (Liou & Kar, 2014).

“Remote sensing provides spatial and temporal information of Normalized Difference Vegetation Index (NDVI), Leaf Area Index (LAI), surface albedo, surface emissivity, and radiometric surface temperature” (Liou & Kar, 2014). However evapotranspiration cannot be directly retrieved using satellite remote sensing. Models are required to estimate ET on the basis of remote sensing products. From 1980 many papers have been published in using land surface temperature (LST) data in remote sensing techniques to estimate evaporation. From 1991 till 1999, Moran and Jackson, Kustas and Norman, Quattrochi and Luval provided overview to use the thermal infrared radiation (TIR) data in ET estimation. In recent years Overgaard et al (2006), Gowda et al (2007) and Glenn et al (2007) addressed the use of remote sensing in estimation approaches from a hydrological perspective, focusing on specific reference to plant sciences applications. In year 2007 Farahani et al introduced remote sensing based measurement, modelling and mapping of crop evaporation for large areas and also in irrigation areas with less extent. In year 2008 Verstraeten et al provided a comprehensive review of ground based and remote sensing based methods for evaporation estimation (Kalma et al., 2008).

2.2. Estimating Actual Evapotranspiration

Remotely sensed methods for ET estimation are physically based models based on the surface energy balance concept. These models assume that the ET process uses the available energy (from net radiation) to vaporize the water. The surface energy balance at the land-air interface can be written by Equation 2-5 and the net radiation is considered as a residual of the soil heat flux, the sensible heat flux, and the latent heat flux:

$$R_n = G + H + LE + S \qquad \text{Equation 2-5}$$

Where G is the soil heat flux [W·m^{-2}], H is the sensible heat flux [W·m^{-2}], LE is the latent heat flux [W·m^{-2}] and S is the storage of energy by the surface [W·m^{-2}]. In most scenarios the storage term is neglected (S=0) as its value is much smaller than the other terms. In that case, the net radiation (R_n) is only partitioned into G, H, and L.

While many remote sensing models (such as SEBAL and SEBS) use the same parameterizations for estimating the net radiation and ground heat flux, they differ in their calculation of the sensible heat flux.

2.2.1. Surface Energy Balance Algorithm for Land (SEBAL)

SEBAL (Bastiaansen, 1998) is an image processing model for ET estimation as a residual of surface energy balance (Liou & Kar, 2014).

$$LE = R_n - G - H \qquad \text{Equation 2-6}$$

Here, LE [W.m^2] is converted to ET [mm.d^{-1}] with dividing it by the latent heat of vaporization (~ 2.45 [MJkg^{-1}]).

SEBAL approach estimates ET as a residual from the surface energy balance equation(Gowda, Colaizzi, Evett, Howell, & Tolk, 2007). Net radiation (R_n) is computed from the short and longwave radiation. Soil heat flux (G) is calculated using the equation proposed by Bastiaanssen, and the sensible heat flux was determined by an iterative solution of standard heat and momentum transport equations (Kite & Droogers, 2000).

Some advantages of SEBAL are: 1) it uses less ground-based data. 2) It corrects atmospheric effects automatically, SEBAL also has some cons: 1) it needs adjustments for calculation over mountainous regions. 2) H is affected by the errors in surface temperatures measurements. 3) Effect of radiometer viewing angle, causes variation in T_s for some images. 4) it requires calibration (Liou & Kar, 2014).

SEBAL has been designed for the regional scale and used widely with satellite and aircraft data over relatively flat landscapes with and without irrigation (Liou & Kar, 2014).

2.2.2. Surface Energy Balance System (SEBS)

SEBS (Su 2002) uses satellite and meteorological data to estimate sensible and latent heat fluxes. The main basis of SEBS are calculation of roughness length for heat transfer, and estimation of the evaporative fraction based on energy balance for upscaling to daily values.

SEBS is capable of estimating evapotranspiration at different scales (local, regional and global) as it uses different similarity theory when using measurements within the Atmospheric Boundary Layer (ABL) or the Atmospheric Surface Layer (ASL).

Land parameters derived by remote sensing and ground-based meteorological measurements are used as inputs in SEBS daily, monthly, and annual evaporation estimation. The advantages of SEBS are: 1) It considers the energy balance at the limiting cases, which minimizes the uncertainty in surface temperature or meteorological variables, 2) For the roughness height it has a formula instead of constant values, 3) It represents parameters associated with surface resistance. 4) SEBS has been widely applied over large heterogeneous areas with MODIS data. As a drawback it needs many parameters that causes inconveniences when data are not readily available (W. J. Timmermans, Kustas, Anderson, & French, 2007) (Liou & Kar, 2014) (Glenn et al., 2007) (Taylor, Jiang, & Islam, 2010).

2.3. Drought concept

Drought is a natural hazard that occurs when water supply cannot meet the water demand. Monitoring impacts of the drought on ecosystems is very difficult, because droughts impacts are slow and have different impacts based on different regions and systems. Also response of hydrological and biological systems to precipitation are different. In addition to precipitation, other factors such as temperature and evapotranspiration play important role in drought development (Vicente-Serrano et al., 2012).

“Drought indicators based on climate data and remote sensing products are at present the best available tools to monitor drought over large regions and time periods”(Vicente-Serrano et al., 2012). In drought impact development assessments several characteristics need to be considered, such as, occurrence probability, severity and spatial coverage (Dietz, Put, & Subbiah, n.d.).

Different studies have been performed on monitoring impacts of agricultural drought on crops. In terms of agricultural drought, water stress has very important role and close relationships exist between water stress and individual crop yields (Kumar & Panu, 1997). In particular the time of occurrence is very important in the agricultural drought risk assessment. It has been proven that each crop growth stage has its own sensitivity to soil moisture stress. For example, several studies have shown that water stress effect on corn is different per growth stage (Easterling et al., 2000). As such temporal resolutions of evapotranspiration for agricultural drought monitoring is very important and observations should preferably be performed at least once per day.

2.4. Drought indices

The best available tools to monitor drought over large regions and time periods are objective indices (Vicente-serrano et al., 2012). Such an Index should 1) Reflect developing dry condition, 2) It shouldn't be depended to specific season and 3) It can be used for global scale not for specific region (Narasimhan & Srinivasan, 2005). As there are many stages of drought development (meteorological drought, agricultural drought and hydrological drought), the used index should be adequate for that particular stage. The various hydrological and meteorological parameters such as rainfall and evapotranspiration (ET) are required. Consequently, there are different drought indices used for water resources management, agricultural drought monitoring and forecasting. First drought indices were based on meteorological data from synoptic observations but using remote sensing based indices improved drought assessment. Indices can be used individually or in combination with other indices. Some of indices are briefly explained below.

2.4.1. Palmer Drought Severity Index (PDSI)

In 1965, Palmer introduced a drought index based on the measurement of the moisture supply departure. It is based on concept of supply and demand of the water balance equation. PDSI is calculated based on precipitation, temperature and average available soil moisture. It means that it doesn't take to account only precipitation deficit. In this index irrigation water is not considered. It is sensitive to abnormally dry or wet weather condition. PDSI is a meteorological index for relatively homogeneous regions. PDSI has got wide acceptance because it is based on water balance model.

2.4.2. Crop-Specific Drought Index (CSDI)

Another index that is used in agricultural drought monitoring is Crop-Specific Drought Index (CSDI). This index is based on the ratio of actual evapotranspiration to potential evapotranspiration. CSDI was developed for different types of crops between 1990 and 1997(Camargo and Hubbard, 1999). Ratio of actual evapotranspiration to reference evapotranspiration is calculated for crop at each growth period. As an advantage of CSDI in drought monitoring is that it is specific crop based. Thus, the CSDI values can be directly linked to drought impact on the specific crops of interest. Therefore the CSDI is good index for agricultural drought. Wilhite (2000) mentioned that using more than one index would be more reliable for decision making. Agricultural crops are so sensitive to soil moisture deficit during growing period. Also there is a time delay between lack of precipitation and occurrence of soil moisture deficit.

Standardized Precipitation Index (SPI)

In 1993, McKee et al. developed the Standardized Precipitation Index (SPI), which is based on precipitation data and calculation of that requires long term monthly rainfall data for 30 years or more (Edwards, 1997). Long term rainfall data fitted to gamma distribution function that is done based on maximum likelihood estimation process (Hayes, Svoboda, Wilhite, & Vanyarkho, 1999). Because probability function in different area with different data has different standard deviation and mean, thus the cumulative probability gamma function is transferred to a standard normal distribution. It is based on precipitation deficit that affects ground water, reservoir storage, soil moisture. Researches showed that the SPI is a good index for detecting severe drought event that occurred in the southern Great Plains and the southwestern United States in 1996 (Hayes et al., 1999). SPI can be used to monitor dry and wet periods in a long time scale (Edwards & Mckee, n.d.). SPI is a good index for early warning of drought. In agricultural drought monitoring because the growth stage is based on days and weeks, so weekly SPI should be calculated (Karavitis et al., 2011). It is less complex than the Palmer index (Edwards & Mckee, n.d.). Simplicity and temporal flexibility are some of advantages of SPI (Hayes et al., 1999).

Table 2-1. Category of SPI values by Mc Kee and Edward

SPI value	
2.0 and above	Extremely wet
1.5 to 1.99	Very wet
1.0 to 1.49	Moderately wet
-0.99 to 0.99	Near normal
-1.0 to -1.49	Moderately dry
-1.5 to -1.99	Severely dry
-2.0 and less	Extremely dry

2.4.3. Water Requirement Satisfaction Index (WRSI)

WRSI is an index based on availability of water for crop during growing season (Frère and Popov, 1979). It is based on actual evapotranspiration and crop water requirement that is calculated from reference crop evapotranspiration and crop coefficient in growing season. WRSI is shown in percent.

Table 2-2. WRSI based drought severity classes

WRSI (%)	Drought severity
80-100	No drought
70-79	Slight drought
60-69	Moderate drought
50-59	Severe drought
<50	Complete crop failure

2.4.4. Water stress ratio

Water stress ratio is calculated using reference evapotranspiration and actual evapotranspiration. This index is used with ETDI. Based on daily ET_a and ET_{ref}, weekly values of each of them is calculated and finally water stress ratio is calculated based on Equation 2-7(Narasimhan & Srinivasan, 2005):

$$WS = \frac{ET_{ref} - ET_a}{ET_{ref}} \qquad \text{Equation 2-7}$$

Where:

WS is weekly water stress ratio and value of that changes between 0 and 1. Zero means no actual evapotranspiration and 1 means actual evapotranspiration occurs at the same level with reference crop evapotranspiration. ET_{ref} is the weekly reference evapotranspiration of crop, ET_a is weekly actual evapotranspiration of crop.

2.4.5. Evapotranspiration Deficit Index (ETDI)

In year 2005 Narasimhan and Srinivasan developed two drought indices, the Evapotranspiration Deficit Index (ETDI) and Soil Moisture Deficit Index (SMDI).these indices are based on evapotranspiration and soil moisture deficits, respectively. These indices have spatial resolution 4km and temporal resolution daily to weekly (Niemeyer, 2008). In these two indices agricultural drought is computed based on long-term weekly normal soil moisture and evapotranspiration data to calculate SMDI and ETDI. ETDI index is based on weekly mean potential and actual evapotranspiration as estimated by the meteorological and hydrological models. There is a good correlation between SMDI and ETDI. Based on spatial and temporal distribution of ET by using ETDI drought index, severity of drought is quantified. ETDI uses water stress ratio in addition to ET. Weekly actual and reference evaporation data is cumulated based on daily data. So weekly water stress ratio is calculated (Narasimhan & Srinivasan, 2005).

In the long period for different years we have water stress ratio for each week, So we have mean, minimum and maximum value of that for each week. Anomaly in water stress ratio for each week is obtainable as Equation 2-8 and Equation 2-9(Narasimhan & Srinivasan, 2005):

$$WS_{A_{ij}} = \frac{MWS_j - WS_{ij}}{MWS_j - minWS_{ij}} * 100 \qquad \text{If } WS_{ij} \leq MWS_j \qquad \text{Equation 2-8}$$

$$WS_{A_{ij}} = \frac{MWS_j - WS_{ij}}{\max WS_{ij} - MWS_j} * 100 \qquad \text{If } WS_{ij} > MWS_j \qquad \text{Equation 2-9}$$

Where:

$WS_{A_{ij}}$ is the weekly water stress anomaly that has range from -100 to +100, MWS is the long term median water stress. -100 water stress anomaly indicate very dry condition and +100 indicates very wet condition. Finally ETDI index is calculated by Equation 2-10 (Narasimhan & Srinivasan, 2005):

$$ETDI_j = 0.5\ ETDI_{j-1} + \frac{WS_{A_j}}{50} \qquad \text{Equation 2-10}$$

2.5. Disaggregation of parameters

Disaggregation is done for providing high resolution map, using low resolution available data. MODIS based ET estimation is with 1km spatial resolution, while with this spatial resolution, heterogeneity of land cover isn't taken to account. For monitoring drought impacts on crops it is needed to consider heterogeneity of land cover. So MODIS based ET estimations is disaggregated using LANDSAT images that provide high spatial resolution.

3. MATERIALS AND METHODOLOGY

3.1. Study Area

The Netherlands is a small (41526 km^2), low and flat country that is located in Western Europe and has common borders with Belgium in the south, Germany in the East and the North Sea in the North West. Longitude, latitude of the centre of the country is 52.3167° N, 5.5500° E respectively. The climate of the Netherlands is mostly influenced by the North Sea and Atlantic Ocean, with cool summers and moderate winters. Temperatures during the day vary from 2°C to 6°C in the winter and from 17°C to 20°C in the summer.

WGS84: Lat = 53.473 °N
UTM: Y= 5924977 m

WGS84: Long = 3.304 °E
UTM: X = 521238m 31N

WGS84: Long = 7.283 °E
UTM: X = 379894 m 32N

WGS84: Lat = 51.183 °N
UTM: Y= 5664880 m

Figure 3-1. Geographic coordinates of the Netherlands

Average annual rainfall over the Netherlands is about 765 mm, as measured by 18 stations spread over the country. A map of the mean evaporation in the Netherlands during 1971-2000 including the position of the 18 precipitation station is presented in Figure 3-2 (Beersma & Buishand, 2007).

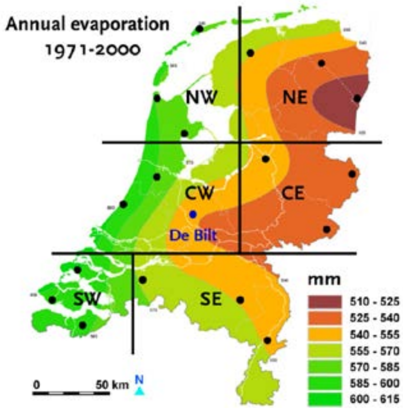

Figure 3-2. Map of annual mean evaporation together with the position of the 18 precipitation stations and the six geographic districts used in this study.

In general average annual precipitation deficit in western part of the country is larger than eastern part (Beersma & Buishand, 2007). As shown in the Figure 3-2 the evaporation in western part is larger than eastern districts and precipitation in eastern districts is larger than western part, although the precipitation deficit is the same in different districts.

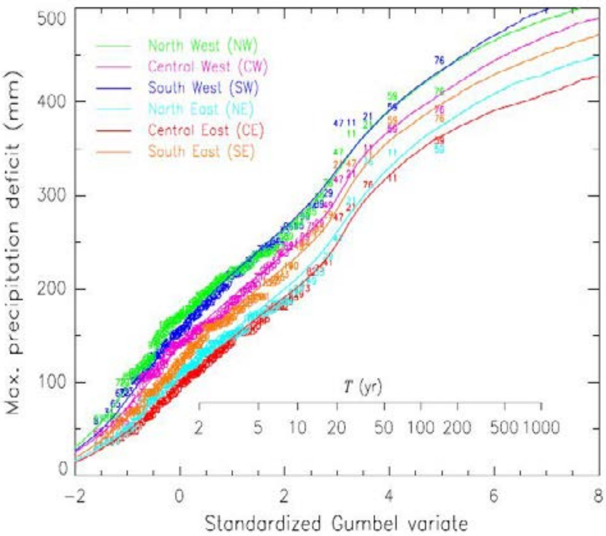

Figure 3-3. Gumbel probability plots of the annual maximum precipitation deficit for the six districts

After the United States, the Netherlands is the biggest exporter of agricultural product in the world ("Agriculture and horticulture | Agriculture and livestock | Government.nl," n.d.). The Dutch agricultural sector exports some € 65 billion of agricultural produce annually, so the agricultural sector plays a crucial role ("Agriculture and horticulture | Agriculture and livestock | Government.nl," n.d.). Based on annual BRP plot registration almost 45% of the fields in the Netherlands are agricultural fields or can be used for agriculture.

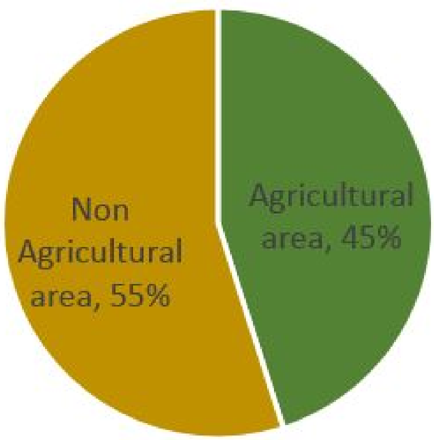

Figure 3-4. Land use segmentation in the Netherlands

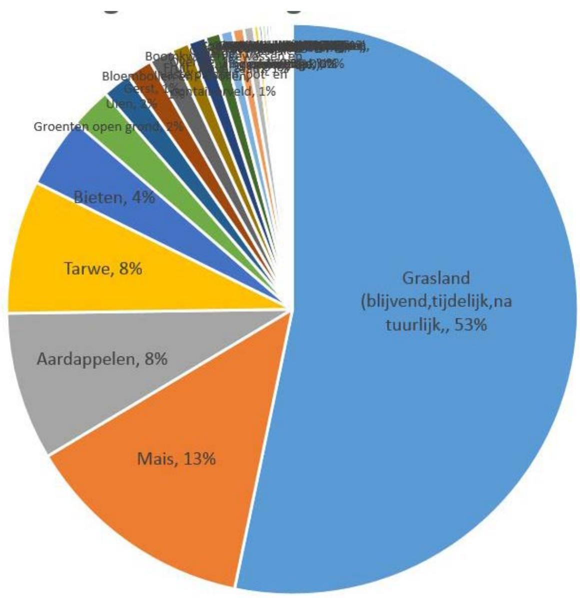

Figure 3-5. Agricultural land cover segmentation

3.2. Data requirements

In order to estimate 1) evapotranspiration, 2) evaluate the accuracies and 3) characterize the heterogeneity of the landscape the following datasets are required:

- For estimating evapotranspiration from the SEBS model, the following data types are needed:
  - Meteorological data from either ground stations or numerical models.
  - Remote sensing based data containing at least land surface temperature observations.
- For evaluating the ET estimates Fluxnet data or Carbo Europe datasets are required.
- For characterizing the spatial-temporal heterogeneity, High resolution land cover maps and high resolution NDVI maps are required.

Each of these data sources is explained in more detail in the following paragraphs.

3.2.1. Meteorological data

Meteorological data can be obtained by ground stations and by numerical models. As specified before, station data has low coverage to be used for large scale evaporanspiration estimation so modelled data is required. The European Centre for Medium-Range Weather Forecasts (ECMWF) is an organization stablished in 1975, supported by 21 European Member States and 13 Co-operating States. ECMWF uses the computer modelling to forecast the weather from its present measured state. The data that provided are:

- Medium-range forecasts, predicting the weather up to 15 days ahead
- Monthly forecasts, predicting the weather on a weekly basis 30 days ahead
- Seasonal forecasts up to 12 months ahead.

Table 3-1. Data gotten from ECMWF for the research

	Description	Unit
H_{abl}	Boundary layer height	[m]
LE	Surface latent heat flux	[W.m^{-2}]
Ns	Sunshine duration	[hour]
P_0	Mean sea level pressure	[kPa]
P_s	Surface pressure	[kPa]
SW_d	Surface solar radiation downward	[W.m^{-2}]
LW_d	Surface thermal radiation downwards	[W.m^{-2}]
T_{dew}	2 meter dew point temperature	[K]
T_a	2 meter temperature	[K]
$W_{U,V}$	10 meter U and V wind components	[m.s^{-1}]

3.2.2. European Fluxes Database Cluster (CARBO Europe)

European Fluxes Database Cluster is an institute for integration and sharing data of different databases. The database receives and distributes data of fluxes are measured mainly using the eddy covariance technique and other data such as meteorological variables, ancillary data, meta-information acquired in sites involved in EU projects and single sites in Europe, Africa and others continents that decided to share their measurements in the database ("carbo europe," n.d.).

Figure 3-6. Map of flux stations in the Netherlands

Table 3-2. List of CARBO Eourope flux towers in the Netherlands

Site name	Code	City	Organization	Status (Lat / Lon)	Field
Cabauw	NL-CA1	Gouda	Wageningen	51.97100 / 4.92700	Agriculture
Loobos	NL-Loo	Apeldoorn	Wageningen	52.16600 / 5.74300	Forest
Molenweg	NL-Mol	Zevenbergen	Wageningen	51.65000 / 4.63900	Agriculture
Haastrecht	NL-Haa	Stein	Wageningen	52.00300 / 4.80500	Agriculture
Oostward	NL-Waa	Wageningen	Wageningen	52.83100 / 4.90900	Agriculture
Vredepeel	NL-Vre	Deurne	Wageningen	51.53100 / 5.84400	Agriculture
Langerak	NL-Lan	Stein	Wageningen	51.95300 / 4.90200	Agriculture
Lutjewad	NL-Lut	Borkun	Wageningen	53.39800 / 6.35600	Agriculture
Dijkgraaf	NL-Dij	Arnhem	Wageningen	51.99200 / 5.64500	Agriculture
Reeuwijk	NL-Re	Rotterdam	Wageningen	51.90000 / 4.50000	Agricultural
Zeewolde	NL-Zee	Almere	Wageningen	52.33400 / 5.37200	Agriculture
Lelystad	NL-Lel	Lelystad	Arjan Hensen	52.52400 / 5.55100	Agriculture
Horstermeer	NL-Hor	Utrecht	Univ_Amsterdam	52.24000 / 5.07100	Agriculture

Different data such as Soil heat flux (G), Sensible heat flux (H), Latent heat flux (LE), Surface thermal radiation downwards (LW_d), NetRad (R_n), Mean sea level pressure (P_0), Surface pressure (P_s), Air temperature (T_a), Surface temperature (T_s), Surface solar radiation downward (SW_d) was obtained for the stations mentioned in Table 3-2. Flux data that gotten is for every 30 minutes. It is necessary to mention that each site has data for some years in period 2002 – 2014. Data availability is shown in the Table 3-3.

Table 3-3. Data availability of flux sites for different years

country	Site code	Site name	Latitude	longtitude	2002	2003	2004	2005	2006	2007	2008	2009	2010	2011	2012	2013	2014
Netherlands	NL_Ca1	Cabauw	51.971	4.927		■	■	■	■	■	■	■	■	■	■	■	
	NL_Hor	Horstermeer	52.24035	5.0713			■	■	■	■	■			■			
	NL_Lan	Langerak	51.9536	4.9029				■	■								
	NL_Loo	Loobos	51.66581	5.743556	■	■	■	■	■	■	■	■	■	■	■	■	
	NL_Lut	Lutjewad	53.3989	6.35602					■	■							
	NL_Mol	Molenweg	51.65	4.639				■	■								
	NL_Haa	Haastrecht	52.00361	4.8055		■	■										
	NL_Dij	Dijkgraaf	51.99206	5.64594						■							
	NL_Vre	Vredepeel	51.5316	5.84411				■	■								
	NL_Waa	Oostwaard	52.8315	4.9091							■						
	NL_Zee	Zeewolde	52.3348	5.3725							■						

In the Table 3-3 the year for which data was available filled in gray.

3.2.3. Land cover data

Every year in the Netherlands information about types of crops that farmers plant at their farm fields is collected at Basis Registratie Percelen organization (BRP). For this thesis Land Cover and Land Use maps for years 2002 till 2014 have gotten from BRP. Data of BRP are used for disaggregation of MODIS product to higher spatial resolution by using LANDSAT images.

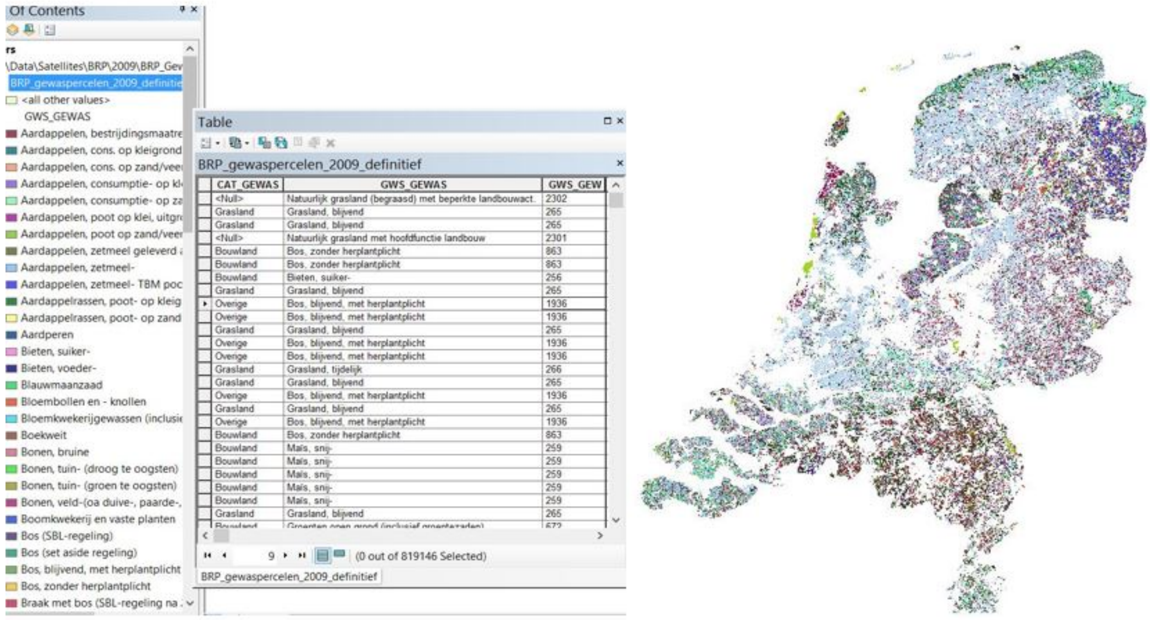

Figure 3-7. Sample of land cover data gotten from BRP

3.2.4. Satellite based data - MODIS data for ET estimation

Different satellites with different spatial temporal resolution can be used for ET estimation but the most common satellites that is used for ET estimation are MODIS and LANDSAT. Data can be downloaded from USGS (http://earthexplorer.usgs.gov) or (http://modis.gsfc.nasa.gov).

Table 3-4. Data from MODIS satellite for ET estimation

variable	Description
α	Albedo
$NDVI$	Normal Difference Vegetation Index
LST	Land Surface Temperature
LAI	Canopy total Leaf Area Index

3.2.5. Satellite based data – LANDSAT images

Landsat images are used to get the NDVI map based on Red and NIR bands and calculate NDVI value. Other bands may be used to control the output results. Data can be downloaded from USGS (http://earthexplorer.usgs.gov)

Table 3-5. Some specification of LANDSAT products

Satellite	**Spatial Resolution**	**Temporal Resolution**	**Red Band**	**NIR Band**	**Altitude**	**Launch Date**
LANDSAT 5	30-120m	Every16days	3	4	705km	1984
LANDSAT 7	30-60m	Every16days	3	4	705 km	1999
LANDSAT 8	15-30m	Every16days	4	5	705km	2013

3.3. Methodology

3.3.1. Flowchart

The whole procedure followed in this research for monitoring impacts of drought on crops via high resolution ET estimation is shown in the chart below (Figure 3-8):

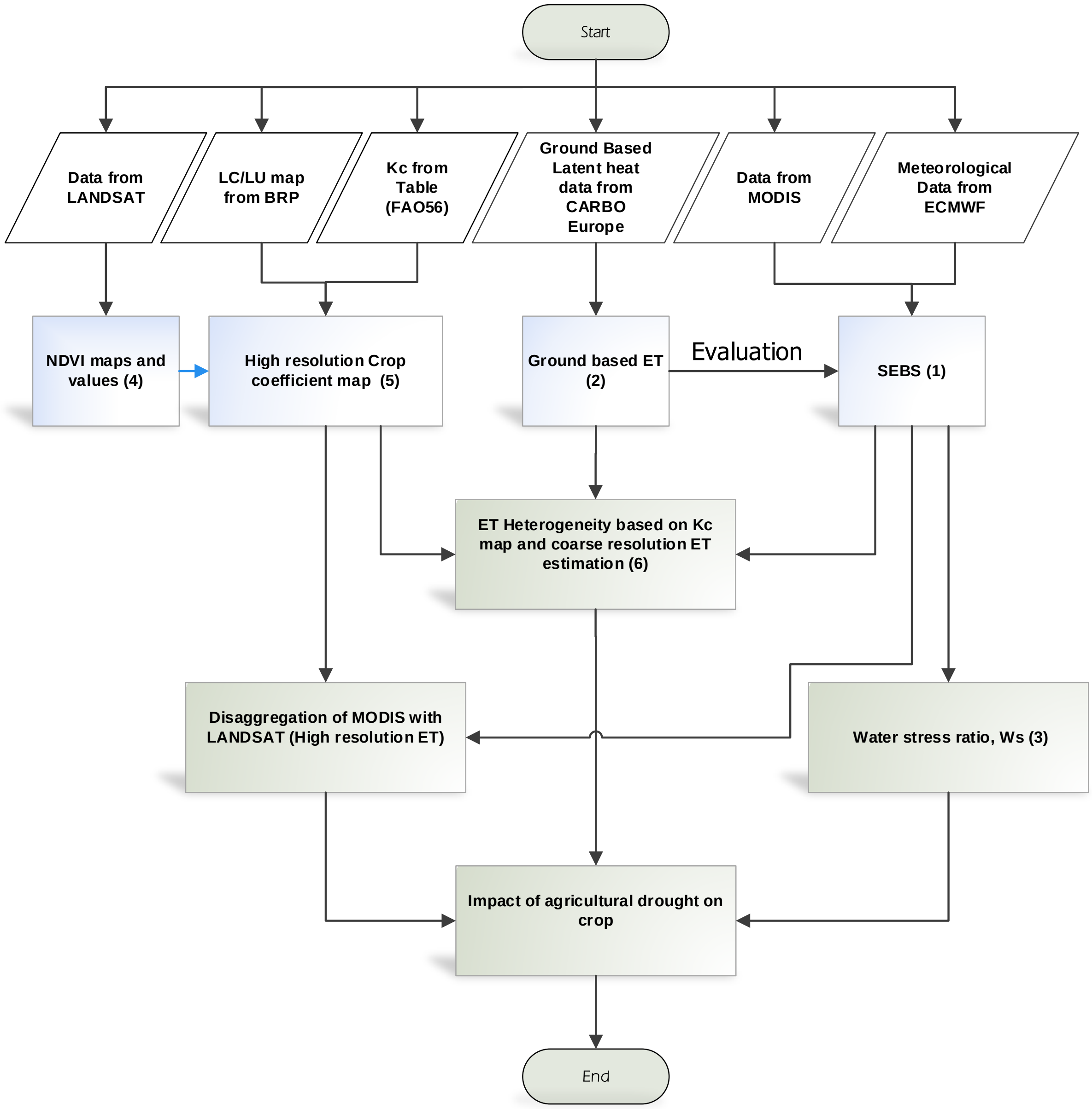

Figure 3-8. Schematic procedure of the research

3.3.2. Actual Evapotranspiration by SEBS

Surface Energy Balance System (SEBS) method is based on 3 main bases: (Liou & Kar, 2014)

- Land surface physical parameters
- Roughness length for heat transfer
- Evaporative fraction

Three most basic inputs required by SEBS are:

- Land surface parameters obtained through remote sensing (albedo (α), Leaf area index (LAI), land surface temperature (LST), emissivity (ε), surface roughness (rah) and vegetation height.
- Meteorological data such as air temperature, air pressure, humidity, wind speed at reference height, Boundary layer height, Sunshine duration, mean sea level pressure.
- Downward short wave solar radiation and downward long wave radiation

The SEBS method (Su, 2002) is based on the energy balance equation (see Equation 3-1)

$$R_n = H + G + LE \qquad \text{Equation 3-1}$$

Where:R_n is net radiation [$W.m^{-2}$], G is soil heat flux [W.m^{-2}], H is the turbulent sensible heat flux [W.m^{-2}] and LE is the turbulent latent heat flux [$W.m^{-2}$].

$$R_n = (1\text{-}\alpha)\, SW_d + \varepsilon LW_d - \varepsilon\, \sigma\, T_0^4 \qquad \text{Equation 3-2}$$

Where: α is the albedo, SW_d is the downward solar radiation[$W.m^{-2}$], LW_d is the downward long wave radiation [$W.m^{-2}$], ε is the emissivity of the surface, σ is the Stefan-Bolzmann constant 5.67 *10^{-8} [$W.m^{-2}.K^{-4}$], and T_0 is the surface temperature [K].

$$G = R_n.\ (f_{veg}\ .\ \Gamma_{veg}\ + (1\text{-}f_{veg}\ ).\ \Gamma_{soil}) \qquad \text{Equation 3-3}$$

Where: f_{veg} is the fraction of the soil that is covered with vegetation and Γ_{veg} is ratio of soil heat flux to net radiation that is equal to 0.05 for full vegetation canopy and Γ_{soil} = 0.315 is for bare soil.

$$H = \rho.\ C_p\ \frac{(Ts - T_a)}{rah} \qquad \text{Equation 3-4}$$

Where: ϱ is the density of air =1.2 [$kg.m^{-3}$], Cp is the specific heat per unit mass =1004 [J. $kg^{-1}.K^{-1}$], T_s is surface temperature, T_a is the air temperature and rah is the surface roughness.

In SEBS method in dry condition the latent heat flux is zero and in the wet condition sensible heat flux will be in minimum range (Liou & Kar, 2014). Most of the time estimation of ET is for daily time scale, but the problem is, sensible heat flux and as a consequence latent heat flux are calculated at the time when satellite overpass. So for extrapolating instantaneous ET estimation, Evaporative Fraction (EF) is used asEquation 3-5.(Glenn et al., 2007).

$$EF = \frac{LE}{R_n - G} \qquad \text{Equation 3-5}$$

3.3.3. Evaluation of evapotranspiration estimations

Evaluation of coarse spatial resolution ET map was done by using ground based measurements on the basis of the Root mean square errors (RMSE) between the observation and the measurement.

$$RMSE = \sqrt{\frac{\sum_1^n \quad (ET_{SEBS(n)} - ET_{Obs(n)})^2}{N}} \qquad \text{Equation 3-6}$$

ET_{SEBS} is the daily ET estimations based on SEBS method [mm $.day^{-1}$] . ET_{obs} is daily ET estimations based on ground based data [mm $.day^{-1}$]. N is the number of days. Yearly evaluation for years 2002 till 2013 was done for each station.

3.3.4. Drought severity estimation

After evaluation of ET, weekly water stress ratio (Ws) was calculated by using Equation 2-7, as mentioned in section 2-4-5 water stress ration is used for ETDI calculation for measuring drought severity.

3.3.5. Characterization of Subpixel heterogeneity

The low resolution actual evapotranspiration obtained through the SEBS represents the total evaporation from different land cover types, inside one individual MODIS pixel. Where the actual evapotranspiration of individual crops can be determined usingEquation 3-8. This crop coefficient can be determined on basis of FAO table data which represents the water demand for different growth stage, as illustrated by Figure 3-10.

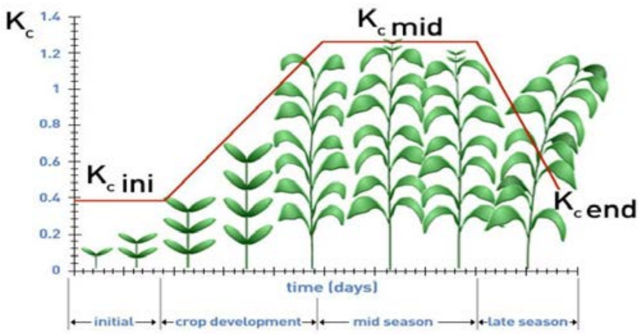

Figure 3-9. Crop coefficient curve from FAO-56, (FAO - Food and Agriculture Organization of the United Nations, n.d.) (Allen, 2000)

The estimation of the crop coefficients therefore depends on: the land cover of the specific pixel and the growth stage of the specific land cover. For land cover information the Basis Registration Products (BRP) is required. For the determination of the growth stage, high resolution NDVI values were used from Landsat. In the past Kc maps have been successfully created for larger area assessments(Bausch, 1995), using shortwave vegetation indices (VIs) such as the Normalized Difference Vegetation Index (NDVI).

(Masek, Schwaller, & Hall, 2006). Kc and NDVI relation should determine empirically by using local ET measurement (Liu, Xin, & Liu, 2009) (Wright, Allen, Tasumi, & Trezza, 2005). Based on the studies done by (Babuaro Kamble, et al 2013) there is a relationship between NDVI and crop coefficient in irrigated and rain-fed agricultural area. The Equation 3-7 describe this relationship (Baburao Kamble, 2013).

$$Kc_{NDVI} = 1.4571\ (NDVI) - 0.1725$$ Equation 3-7

Where 1.457 and 0.1725 represent the slope and intercept coefficients. It is necessary to mention that Equation 3-7 can be used only for irrigated and rain-fed agricultural areas and not for the other type of land covers (Baburao Kamble, 2013).

3.3.6. Disaggregation ET map to high temporal spatial resolution

When subpixel heterogeneity of a MODIS pixel is characterized, it is possible to disaggregate the coarse evapotranspiration estimation to higher resolutions. Scaling of satellite products can be performed by satellite products with different spatial and temporal resolutions.

The total evapotranspiration of a pixel can be considered as the summation of contributions of all the land cover classes contained in that pixel.

$$< ET_a > = sum\ ET_a(i)$$ Equation 3-8

As mentioned before ET can be estimated by using crop coefficient,that provides high resolution ET estimation. Equation 3-9determines high resolution ET estimation based on crop coefficient.

$$ET_{HR} = ET_{ref} \,.\, K_{c_{HR}} \,.\, K_{s_{HR}}$$ Equation 3-9

Where the Ks is the crop stress coefficient. A weighing map can be obtained so that coarse resolution evapotranspiration estimations can be up-scaled to higher resolutions.

$$ET_{HR} = W_{HR} \,.\, ET_{LR}$$ Equation 3-10

$$W_{HR} = \frac{\mathrm{K_{cHR}K_{sHR}}}{\langle \mathrm{K_{cHR}K_{sHR}} \rangle}$$ Equation 3-11

The estimation of this weighing kernel can be simplified if the crop-stress coefficients within the coarse resolution pixel are considered homogeneous.

$$W_{HR} = \frac{\mathrm{K_{cHR}}}{\langle \mathrm{K_{cHR}} \rangle}$$ Equation 3-12

3.3.7. Evaluating ET and drought status for individual crops

WS for crop in previous drought years is measurable and the crop behavior in different values of WS can be monitored. The result will help to collect statistics about what is the minimum and maximum value for a specified type of crop in each plot and the range of WS value in different drought conditions. It helps to provide information that would be useful and applicable in terms of agriculture and water management for decreasing the losses in drought events.

3.3.8. ET mapping with NDVI:

$$ET_p = K_c \,.\, ET_{ref}$$ Equation 3-13

4. DATA PROCESSING

Because of huge data set that is for 12 years for whole entire the Netherlands, data processing and as a consequent doing this research manually wasn't possible. So automatic way using MATLAB was selected.

4.1. ET estimation by SEBS

As mentioned in the methodology section, SEBS model was used to estimate actual evapotranspiration by using MODIS and meteorological data. For using SEBS model some inputs are needed:

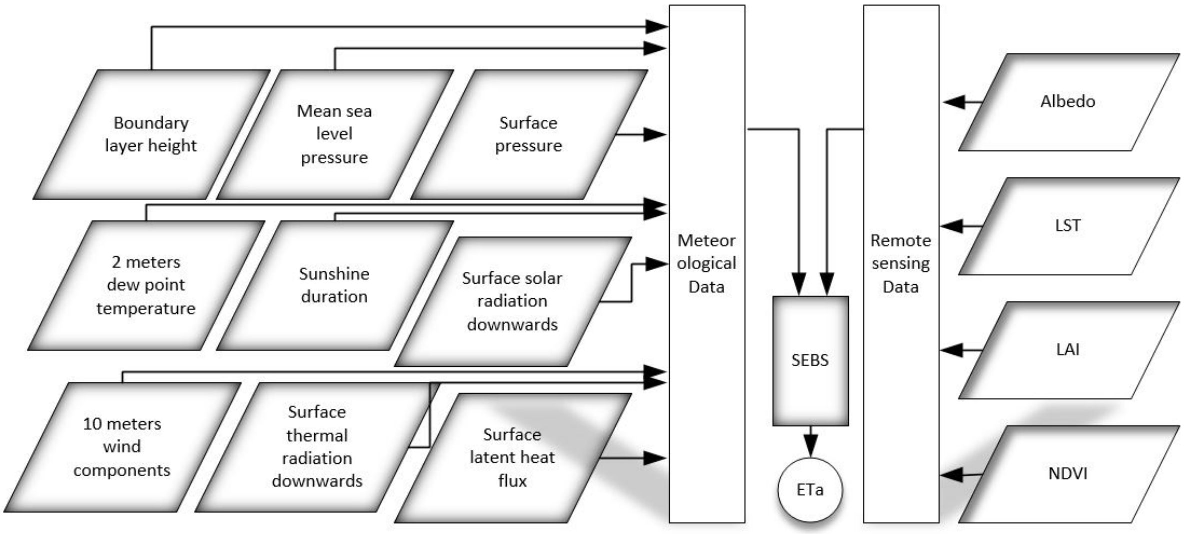

Figure 4-1. Schematic chart for data used in SEBS model

A part from introduced variables and parameters also there are another data those are needed for calculating H,G, R_n in SEBS. These inputs are calculated by using preliminary inputs:

For calculation of G_0 the Equation 4-1 is used while in this equation f_c that is fractional canopy coverage is not introduced that can be calculated by Equation 4-2.

$$G = R_n . [\Gamma_v + (1 - f_c). (\Gamma_s - \Gamma_v)]$$ Equation 4-1 (Su, 2002)

G is soil heat flux , R_n is net radiation , Γ_v is Ratio between Rn and G for vegetation and Γ_s is Ratio between R_n and G for soil. The values of Γ_s and Γ_v are 0.315 and 0.05 (Su, 2002). f_c is calculated with Equation 4-2

$$f_c = 1 - \left(\frac{NDVI - NDVImax}{NDVImin - NDVImax}\right)^k$$ Equation 4-2 (Su, 2002)

Where: k = 0.4631.

For calculation of sensible heat flux, variable L that is Monin-Obokhov length is needed and is calculated based on Equation 4-3

$$\text{Monin – Obokhov length L} = \frac{\rho \;\; C_p \;\; u_*^3 \; \theta_v}{K \; g \; H} \qquad \text{Equation 4-3}$$

ρ is air density, C_p is specific heat capacity, $u_*$is friction velocity, θ_v is virtual potential air temperature

$$u_* = \frac{K \;\; U_{ref}}{\log \frac{Z-do}{Z_{0m}}} \qquad \text{Equation 4-4}$$

$$\theta_v = \theta_a \; (1 + 0.6 \; . \; q_{ref}) \qquad \text{Equation 4-5}$$

Also evaporative fraction should be defined. For defining that energy balance considered at limiting cases. Under dry limit latent heat (LE) is zero and sensible heat (H) is maximum (Su, 2002). In wet limit latent heat occurs at potential rate and sensible heat has its minimum. Finally evaporative fraction can be defined as below: (Su, 2002)

$$\Lambda = \frac{LE}{R_n - G} \qquad \text{Equation 4-6}$$

4.2. Evaluation of evapotranspiration using Carbo Europe data

After getting the outputs of daily evapotranspiration based on SEBS model, to check the accuracy of the outputs, evaluation of the results was done with ground based data. CARBO Europe data were used as reference. However this data are available for every 30 minutes. So for each day 48 instantaneous measurements should be available, while because of the weather condition particularly in the Netherlands, for some days there are less than 48 measurements per day. Instantaneous measurements need to be processed to daily values in order to do the evaluation of evapotranspiration estimation data.

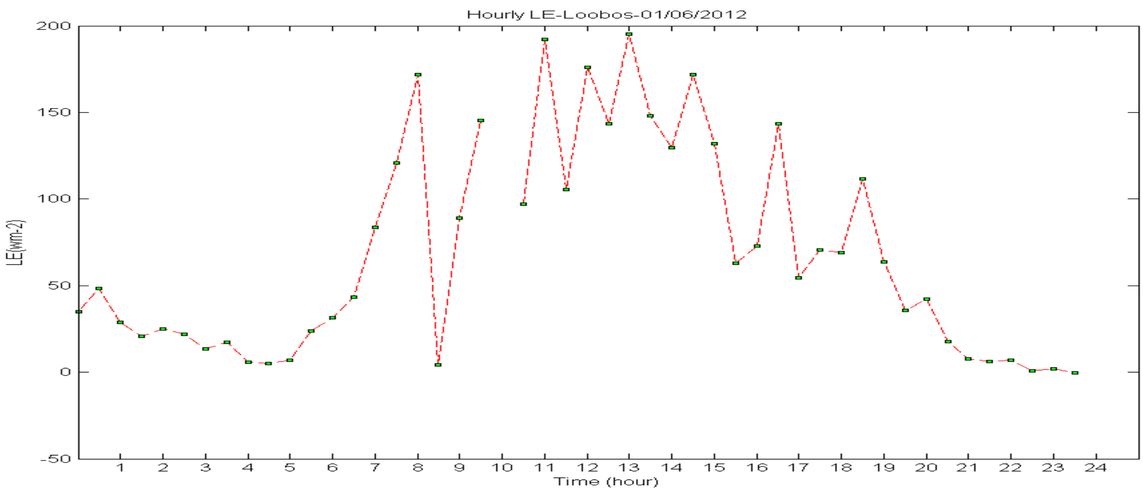

Figure 4-2. Hourly Latent heat flux for one day, calculated based on instantaneous measurements

Gaps in the plot shows particular times for those there wasn't adequate data.

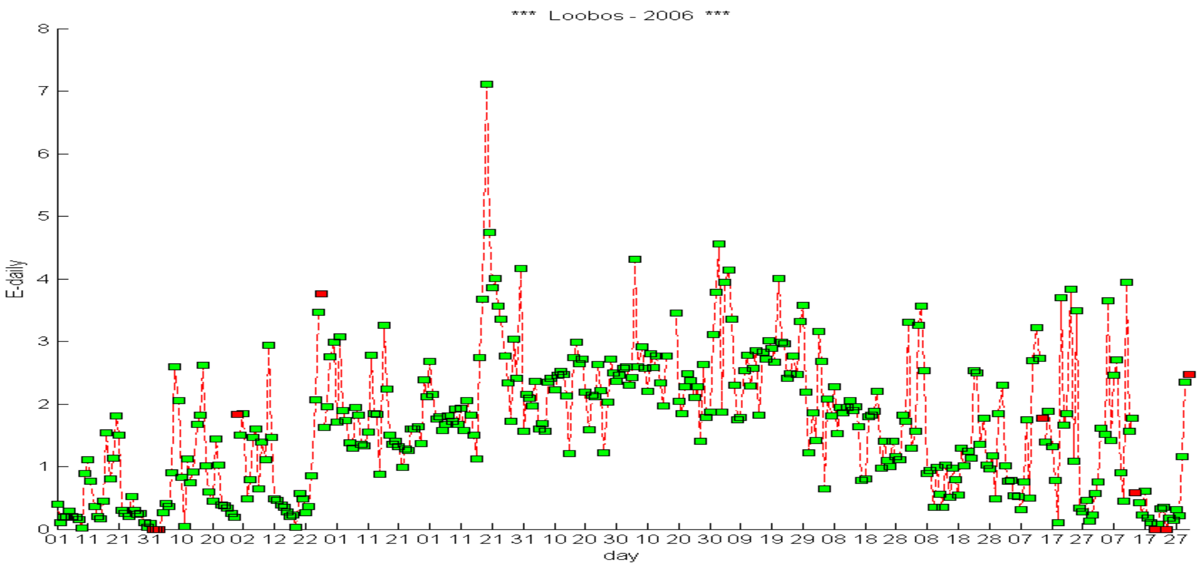

Figure 4-3. Daily evaporation for Loobos station for year 2006

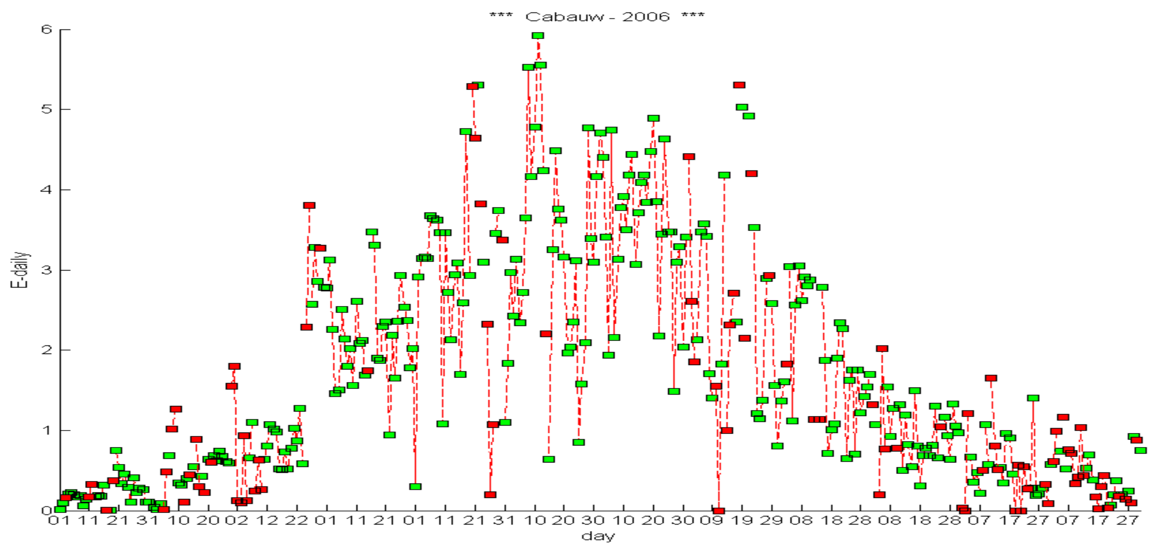

Figure 4-4. Daily evaporation for Cabauw station for year 2006

In Figure 4-3 and Figure 4-4 for some days, ET is shown by red color mark. In these days the number of latent heat flux measurements were less than 50%. It means the number of observations was less than 24 observations for all the day. ET estimation of these days weren't take into account in SEBS evaluation.

After the daily evapotranspiration estimations from carbo Europe have been determined, they were compared against the actual evapotranspiration by SEBS. One example is shown in Figure 4-5.

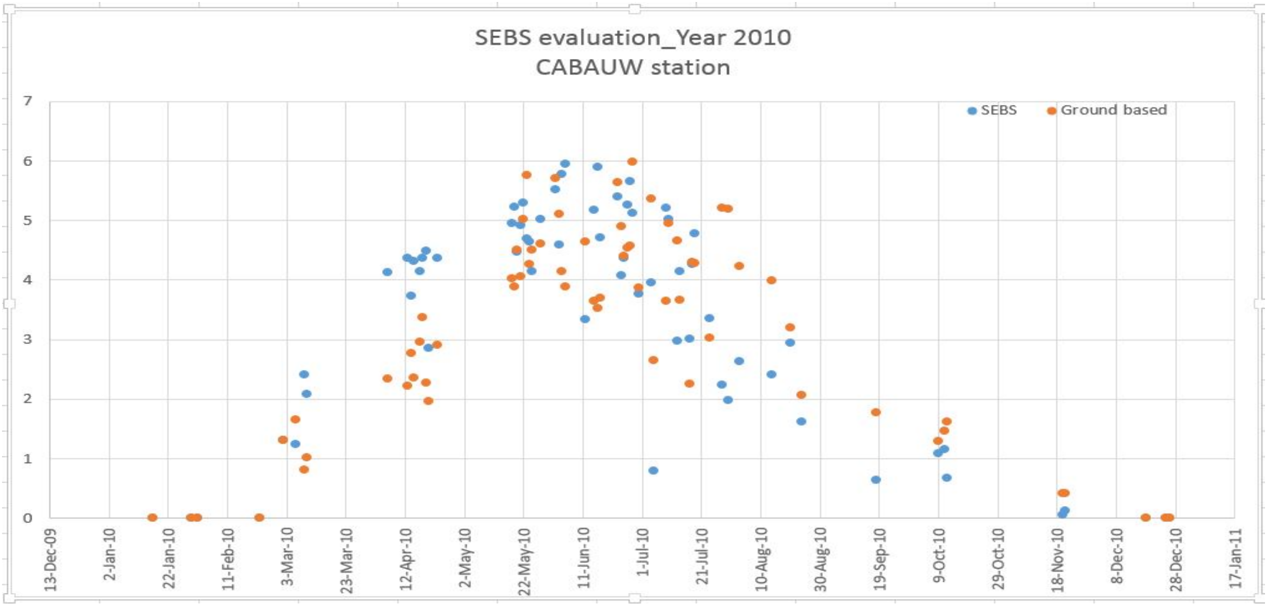

Figure 4-5. Evaluation of SEBS estimation in CABAUW station for year 2010

4.3. Land cover data processing

BRP data have Dutch geographic coordinate system (RD_New). So coordinate conversion from RD_New datum to WGS84 was done. Additionally in order to use BRP data with the evapotranspiration (raster) data, conversion of them from polygons to Raster was needed. During this conversion step, it was investigated which cell size best represents the plots in the Netherlands. The results of this investigation are shown in the results section

Figure 4-6. Coordinate conversion from RD_New datum to WGS84

4.4. LANDSAT images for calculating temporal NDVI

Estimating NDVI from LandSAT data requires several processing steps. These steps are provided in the following paragraphs.

4.4.1. Radio metric correction on LANDSAT images

Digital sensors record the intensity of electromagnetic radiation from each spot viewed on the Earth's surface as a digital number (DN) for each spectral band. The range of DN depends on its radiometric resolution. For example one sensor measures radiation on a 0-63 DN scale while another one measures it on a 0-255 scale. In working with time series satellite images, images are for different atmospheric conditions and different sun angle elevation. The sun elevation angle for the winter is different with for the summer one. So, the DN values recorded for the same area will differ between the two images. So for correcting these effects, radiometric correction is done as procedure shown below:

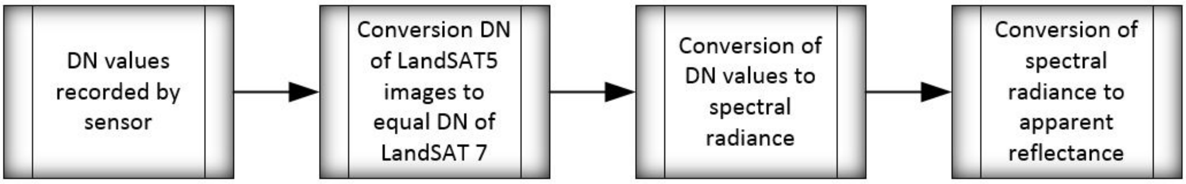

Figure 4-7. The process of radiometric correction of LandSAT images

- **Conversion DN5 to DN7**

  Where: gain and bias are band-specific numbers. L_λ is calculated radiance. DN7 is the digital number of LANDSAT 7 image. For LANDSAT 5 image at first conversion to DN7 is done by Equation 4-7.

  DN7 = ($slope_{\,\lambda}$ * DN5) + $\mathrm{intercept}_\lambda$ Equation 4-7 (Carter, Graham, & Notepad, 2011)

band	slope	intercept
1	0.943	4.21
2	1.776	2.58
3	1.538	2.5
4	1.427	4.8
5	0.984	6.96
7	1.324	5.76

- **Convert DN data to radiance data:**

  DN values should be converted to radiance. This conversion is done by Equation 4-8.

  L_λ = ($gain_\lambda$ * DN7) + $bias_\lambda$ Equation 4-8 (Carter et al., 2011)

band	Gain	Bias
1	0.778740	-6.98
2	0.798819	-7.20
3	0.621654	-5.62
4	0.639764	-5.74
5	0.126220	-1.13
7	0.043898	-0.39

- **Conversion of radiance to reflectance :**

  This conversion removes the differences caused by the position of the sun and the differing amounts of energy output by the sun in each band. Conversion is done by Equation 4-9.

$$R_\lambda = \frac{\pi * L_\lambda * d^2}{E_{sun,\lambda} * \sin(\theta_{SE})} \qquad \text{Equation 4-9}$$

Where: R_λ is the reflectance, L_λ is radiance, d is the earth-sun distance, $E_{sun,\lambda}$ is the band-specific radiance emitted by the sun, and Θ_{SE} is the solar elevation angle.

band	$E_{sun,\lambda}$ (W/m^2µm)
1	1997
2	1812
3	1533
4	1039
5	230.8
7	84.9

In LANDSAT 8 image, reflectance value for each band has given in Meta data file, so this conversion has done directly for LANDSAT 8 image.

4.4.2. Cloud masking:

Clouds have strong effect on reflectance that received by sensor and will cause wrong result especially in calculation of NDVI that is totally based on the reflectance. Because of the weather condition in the Netherlands the number of suitable images that can be used is very less, compared to total images that should be one image for every 16 days. So images with cloud cover less than 60% were selected for the research. Cloud filtering had done by defining maximum and minimum threshold for reflectance in bands RED and NIR. Averaging type of filter selected as a cloud filter. Also by this method shadow effect caused by clouds was corrected.

4.4.3. Stripe masking

In 2003 sensor SLC in LANDSAT7 got off, so from that time there are some stripes in LANDSAT 7 images. Because correction of these stripes and finding a correct value for the pixels on the stripes is very complicated and time consuming process for too many images and wasn't possible at this period of time so value of -1 specified for the pixels in stripe as mentioned in Figure 4-8. Later on during the next processes this value changed to Nan value.

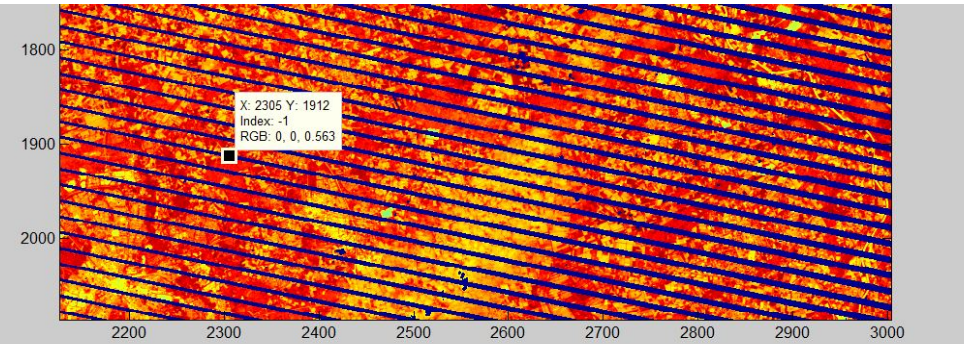

Figure 4-8. Stripe masking process on LandSAT 7 images

After all the process mentioned above, calculation of NDVI was done and the NDVI images were derived. Figure 4-9 shows a sample of derived images.

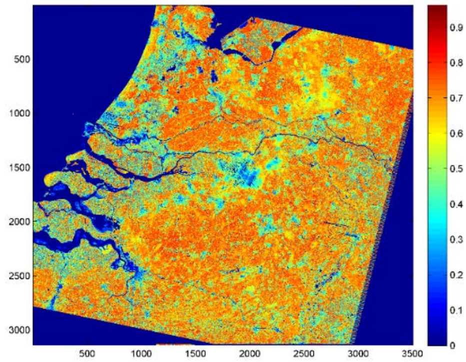

Figure 4-9.Example of obtained NDVI based on LANDSAT images

4.4.4. Aggregation of NDVI images from 30 meters to 60 meters

After calculation of NDVI images based on LANDSAT images, aggregation of them was done because, firstly the resolution of images were 30 meters and doing further processes in this resolution with huge data set with too many images would took lots of time. Secondly in the other hand the cell size of BRP maps was 60 meters so NDVI images aggregated to 60 meters resolution. For this aggregation coincidence of images were too important.

4.4.5. Collocation of Images

It was found that the different Landsat images had different sizes and there wasn't good collocation between them. Images had different sizes and they weren't exactly coincident on each other, especially after aggregation it was necessary to control if they are coincide or not and make correction if is needed. In working with time series it is very important that images been collocated. Therefore after correcting a control was performed in both direction, X and Y. one sample of this collocation process is shown in Figure 4-10

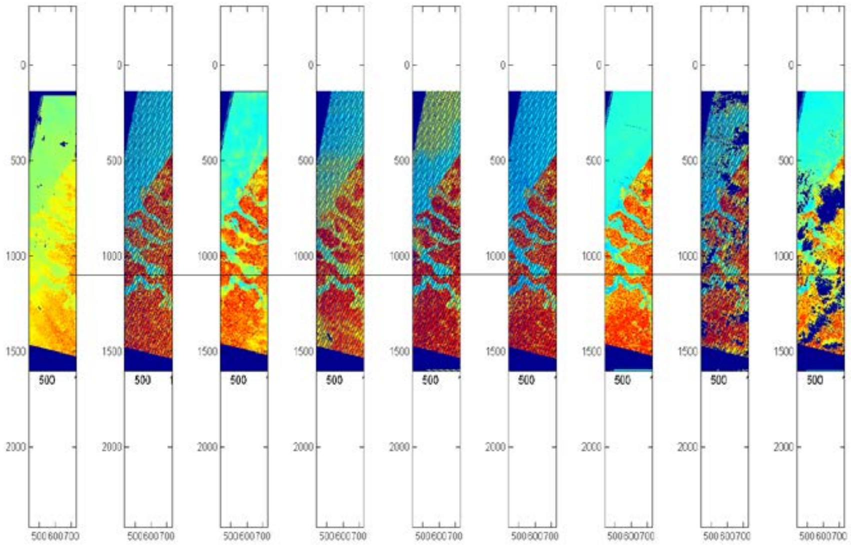

Figure 4-10. Control on NDVI images for being collocated

4.5. Crop Coefficients estimation

4.5.1. Estimating growth stages from NDVI

The growth stage was determined on basis of the temporal NDVI values as obtained by LandSAT images. The starting of the growth of crop is characterized by incrementing values of NDVI. Afterwards the NDVI remains relatively stable during the middle season and finally by starting the end season, NDVI value shows decrement as is illustrated by Figure 4-11.

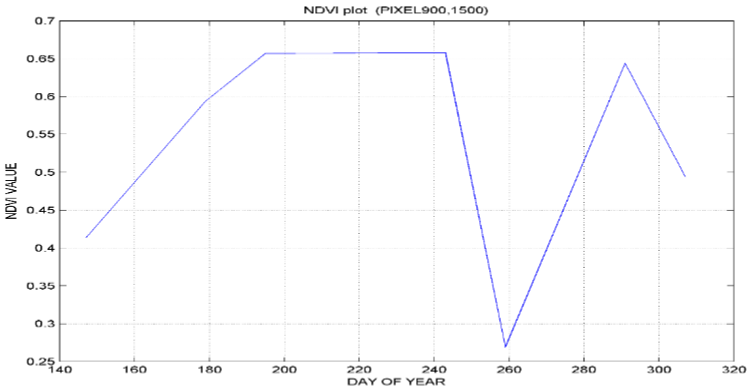

Figure 4-11. NDVI value plot for one pixel

So based on NDVI plot, different steps of crop growth can be derived. It can be seen that because the low temporal frequency of Landsat and because of the weather conditions in the Netherlands, the number of suitable images are very few.

4.5.2. Crop Coefficient table

Before crop coefficient for the different growth stages can be computed, Crop types are derived from BRP maps need to be linked up against crops in the FAO_56 crop coefficient table and NDVI data need to be collocated with the land cover map.

These crop coefficients are listed inTable 4-1. Values for the crops those aren't in the table determined by Equation 3-7 . In terms of the gaps in BRP map, they mostly were residential area and some of those were forest, so it considered in calculation process.

4.5.3. Collocating BRP images with NDVI

For deriving weighting map for disaggregation process, BRP maps and NDVI should collocate. Cutting BRP to the same size with the exact area coordination as NDVI images and make them coincident. This collocation was done for all images for yearly BRP images.

Table 4-1. Kc values for crops of the Netherlands based on FAO_56

Crop	Kc Initial	Kc – Middle	Kc – End	Crop	Kc-Initial	Kc - Middle	Kc – End
Grassland	0.95	1.05	1	Flax	0.7	1.05	0.2
Grass seed	0.9	0.95	0.95	Beans	0.5	1.052	0.9
Corn	0.3	1.15 - 1.2	0.6 – 0.3512	soybeans	0.4	1.15	0.5
sunflowers		1.0 -1.159	0.35	Beets, sugar	0.35	1.2	0.705
Beet, fodder		1.2	0.7	Forest			
Braak	0.25			Mandarin	0.6	0.55	0.6
Onions	0.6	0.95	0.65	Orange tree	0.75	0.7	0.75
Peas	0.5	1.15	1.1	Rye	0.95	1.05	1
Potatoes,		1.15	0.754	alfalfa	0.3	1.15	1.1
oats		1.15	0.25	cereals	0.3	1.15	0.4
Wheat	0.4 – 0.7	1.15	0.25 – 0.41	Opium poppy			
Barley		1.15	0.25	rapeseed		1.0 –1.159	0.35
triticale	0.7	1.15	0.95	walnuts			

4.5.4. Estimating Crop Coefficient maps

After obtaining high resolution NDVI image for each step of crop growth and by using the K_c values gotten from FAO_56 crop coefficient map can be created. Crop coefficient map is used as a weighting map for disaggregation of low resolution ET image (MODIS based ET) to high resolution. For each year 3 high resolution K_c map obtained based on different steps of crop growth.

4.6. Identifying the MODIS subpixel heterogeneity

Each MODIS pixel has 1km spatial resolution, while different type of terrains can be located in 1km*1km area and each of them has effect on actual ET. For considering the impact of heterogeneity on ET, accurate information or suitable data about land cover and land use is needed. Based on the disaggregation effect of heterogeneity on ET can be investigated.

4.7. Water stress ratio processing

Based on SEBS evapotranspiration estimation, actual ET was derived and the result was evaluated with Carbo Europe estimations. Also reference evapotranspirations estimated using Penman-Monteith equation. Weekly actual ET and reference ET calculated and by using the Equation 2-7 water stress ratio derived.

5. RESULTS AND DISCUSSION

5.1. ET estimation results

SEBS based ET estimation was done for all days from year 2002 till 2014 for whole the Netherlands. Two examples are shown in Figure 5-1.

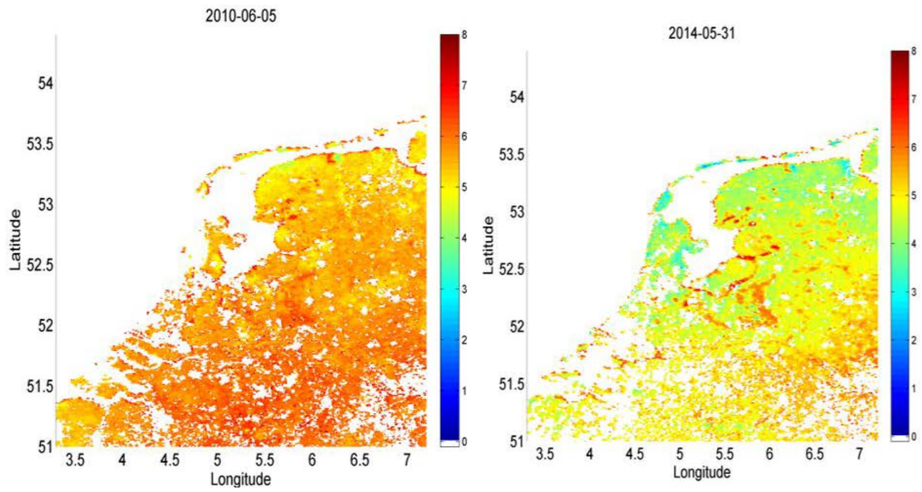

Figure 5-1. Evapotranspiration as calculated by SEBS for two days in 2010 and 2014

As shown in SEBS outputs in figure 5-1 for the water body areas, where there is sea, evapotranspiration is not estimated. Also for some parts because of clouds there is no estimation.

The graphs about the number of SEBS outputs show the average number of output values from SEBS is almost 70 values per year, that is very few compared to 365 days in year. SEBS estimation is done using ground and satellite data, while there are too many cloudy days per year in the Netherlands and this condition strongly affects remote sensing based data.

5.2. Results of ET Evalutation

The evaluation process was done via comparison with the ET estimation of 11 flux stations. The evaluation results are shown in Table 5-1. For drought years 2003 , 2006 and reference year 2005, the evaluation results are shown in Figure 5-2.

Table 5-1. RMSE and number of SEBS values in ET evaluation

Site name	2002		2003		2004		2005		2006		2007		2008		2009		2010		2011		2012		2013	
	RMSE	Numbers	RMSE	Numbers	RMSE	Numbers	RMSE	Numbers	RMSE	Numbers	RMSE	Numbers	RMSE	Numbers	RMSE	Numbers	RMSE	Numbers	RMSE	Numbers	RMSE	Numbers	RMSE	Numbers
Cabauw			0.681	101	0.572	69	0.527	72	0.537	75	0.551	67	0.466	68	0.485	80	0.501	75	0.512	86	0.433	74	0.551	61
Horstermeer					0.36	61	0.535	68	0.398	66	1.158	61	0.601	70					0.655	75				
Langerak							0.582	79	0.146	74														
Loobos	0.82	54	1.142	71	0.753	39	0.804	46	1.011	53	0.999	59	0.842	50	0.865	55	1.128	54	0.976	61	0.753	40	0.89	51
Lutjewad									0.405	65	0.575	64												
Molenweg							0.702	64	0.286	70														
Haastrecht			0.353	103	0.276	62																		
Dijkgraaf											0.461	65												
Vredepeel									0.791	59	0.346	68												
Oostwaard													0.593	91										
Zeewolde													0.757	79										

Figure 5-2. Evaluation of actual ET estimations of SEBS with ground based estimation in flux stations

As shown in Figure 5-2 and Table 5-1only for the Loobos and Horsermeer RMSE values are more than 1.0

- As can be seen in Figure 3-6(Map of flux station) Loobos flux station is located in a forested area and it has been shown in the past that SEBS (similar to other remote sensing models) have problems with estimating ET for such vegetation types (J. Timmermans et al., 2014)
- Another problem is that the Horstermeer station shows fluctuation in the root mean square value. It means for some years it has a less error while for others the value is high. This station is located

near the water body. As SEBS version was not designed for open water evaporation, it can be concluded that the water body affects the ET estimation at this station. Additionally, research has been done on updating SEBS to incorporate open water body (Abdelrady, 2013).

While the other stations show good accuracies (with RMSE values <1), disaggregation of these values might in fact increase these results further. As such subpixel heterogeneity of these coarse resolution values is performed in the following paragraph.

5.3. Land cover data processing results

Land cover heterogeneity was investigated based on the land cover maps gotten from BRP. For considering heterogeneity in drought monitoring, the land cover cell size should be coincide with the high resolution NDVI images. Based on the result of investigation which is shown in Table 5-2 suitable cell size for land cover maps in converting them to the raster is 50m*50m.as shown this cell size covers 90% of plot sizes in the Netherlands and only 10% isn't covered. Although 30m*30m cell size has better coverage, it causes much more computation process in disaggregation. Each individual NDVI images had 30m*30m cell size and after aggregating them this value changed to 60m*60. So finally for the BRP maps 60m*60m cell size was chosen.

Table 5-2 . Analyzing for suitable cell size in converting BRP map from polygon to raster

Year	Number of all Polygons	Number of polygons<900 m²	percent< 30*30	Number of polygons<2500 m²	percent< 50*50	Number of polygons<8100 m²	percent< 90*90	Number of polygons<62500 m²	percent< 250*250
2009	819146	30131	3.68	86959	10.62	238840	29.16	765850	93.49
2010	782837	22046	2.82	68593	8.76	210097	26.84	729315	93.16
2011	779674	21974	2.82	68697	8.81	209805	26.91	726519	93.18
2012	772865	22176	2.87	68652	8.88	207646	26.87	719479	93.09
2013	762725	21348	2.80	66714	8.75	203933	26.74	709622	93.04
2014	770061	22919	2.98	70439	9.15	209736	27.24	715932	92.97

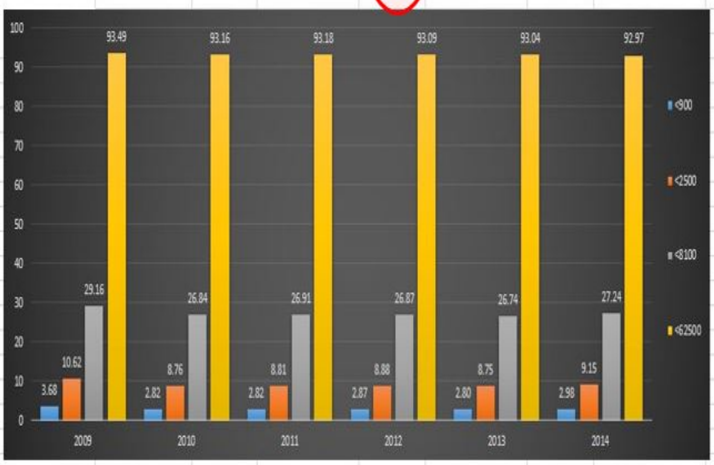

Another correction that done on BRP images was gap fill. For some area there was no information about land cover maps, so for using them in disaggregation process it was necessary that each pixel has value. So based on different land cover product from other sources like MODIS images suitable value assigned to the pixels that there was no data for them on BRP maps.

5.4. LANDSAT images for calculating temporal NDVI

For monitoring impact of water stress and drought on crops, ET estimation should be done on coincident resolution with plot sizes. For investigating the subpixel heterogeneity of MODIS data, crop coefficients needed to be determined. This can be done if BRP data is collocated with the NDVI data from Landsat.

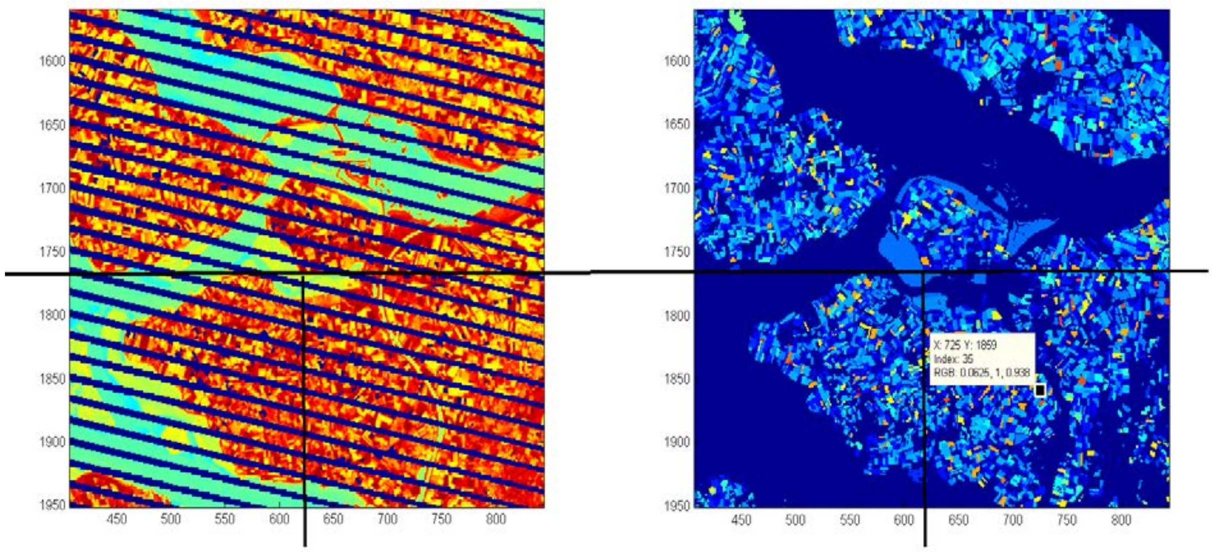

Figure 5-3. Collocation of NDVI and BRP

As shown in Figure 5-3 BRP maps and NDVI images strictly collocated to each other. It can be seen that for each type of land cover NDVI value can be obtained. So this lead to considering heterogeneity in ET estimation and drought monitoring.

After the collocation of the BRP with the different NDVI images has been accomplished, the growth stages can be determined.

5.5. Growth stage estimation results

In the Netherlands there are different crops, so that each of them can have different growth period. These start and end dates therefore need to be determined. For reaching this objective average NDVI (per crop) was derived as shown in Figure 5-4.

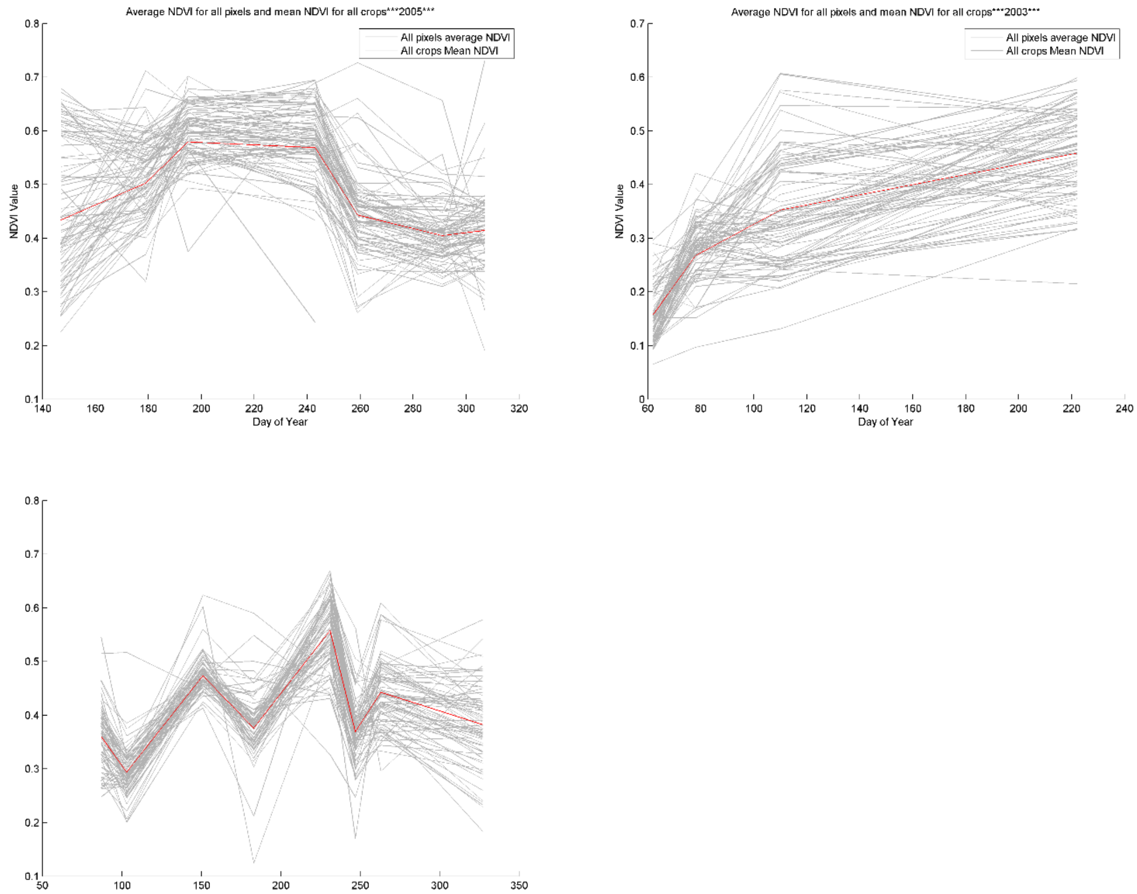

Figure 5-4. Average NDVI for all pixels and mean NDVI for all crops

It was observed that 2005 was the year with the most clear sky observations. Therefore the initial study focused on obtaining crop coefficients for this year. However even in 2005, only 12 observations were made (due to the low temporal resolution of Landsat with a revisit time of 16 days, and cloudy conditions). For some years such as 2003 the growth complete process couldn't be obtained because after day 220 there wasn't suitable high resolution image that can be used. So because of this limitation the process continued with the specific years like 2005. In year 2005 as shown in Figure 5-4, crop start and end of growth stages for different plants are the same. In order to improve therefore the growth curve, a mean value (of the whole image) is considered.

Also in contrast to 2005, for year 2012, the different steps in grow seasons are not clear. As mentioned before, in the Netherlands there are too many cloudy days, so that this clouds cause severe problem in remotely sensed gotten data. So for years such as 2003 and 2012 there weren't enough suitable images from LANDSAT so that total images that gotten were for only 98 days for whole the period of 12 years and among them still there were some that were useless because of too much cloud effect.

5.6. Result of Heterogeneity investigation

Based on investigation that was done on BRP maps, plot sizes in the Netherlands are small. Table 5-2 shows that for covering almost 90% plot sizes the resolution of 60m * 60m is needed. In ET estimation by using MODIS data, each cell gives ET mean for 1km * 1km that covers lots of different terrains on the ground, but for all of them ET value is the same. By doing disaggregation and getting high resolution ET in one hand and having accurate land cover map in the other hand, monitoring impact of drought on each type of crops can be done.

For doing investigation on heterogeneity, the location of flux stations were taken into account. In the location on each station, by considering 1km as a resolution, for some of them there are different terrains such as different type of crop plots or water body, residential area and forest. Each of these terrains has its own effect on ET estimation while in coarse resolution estimation, there is one value for all that is mean value.

Result of investigation on heterogeneity of location of stations with 1km foot print are explained below:

- **Oostwaard:** station is located in agricultural field with different crops while it is near the sea. It is not so closed to sea but it is affected by that.
- **Lutjewaad**: in agricultural field. There is a canal in nearby and it can be considered affected by the sea, but not close to that.
- **Lelystad:** located in agricultural area and near water body and residential area.
- **Zeewolde:** the same situation with the Lelystad.
- **Horstermeer** same with the situation Lelystad.
- **Loobos:** is located in the forest area**.**
- **Reeuwijk:** located in crop field in residential vicinity near the port.
- **Dijkgraaf:** in agricultural field near the forest and residential area.
- **Langerak:** in agricultural field and a river is nearby.
- **Cabauw:** in agricultural field and near the river.
- **Haastrecht:** located in agricultural field and a canal is around.
- **Molenweg:** crop field while located in residential area and near the river.
- **Vredepeel:** it is located in agricultural field.

By collocation of land cover map with high resolution satellite images finally the heterogeneity of land cover that causes the heterogeneity in ET estimation is completely considerable. As shown in Figure 5-5 high resolution crop coefficient map obtained from this process that can be used in disaggregation process as weighting map. In coarse resolution ET estimation characteristic of crops in known in resolution 1km*1km. it means each 1km*1km considers as a homogeneous while in reality and as shown in Figure 5-5 and Table 5-3 each type of crops shows different behavior in each stage of growth.

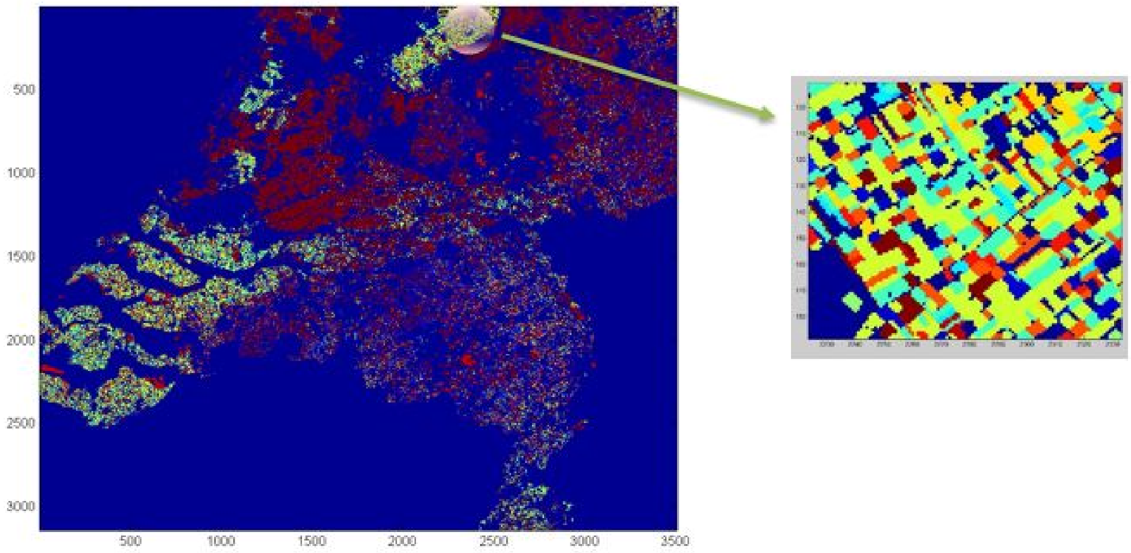

Figure 5-5. High resolution crop coefficient map

As a quantitative result Table 5-3, Table 5-4, Table 5-5 and Table 5-6 show that for each type of crops and for each growth stages Kc value is obtained that is leads to completely know the heterogeneity of the study area. At the end by having the accurate ET estimation and heterogeneity of land cover, monitoring the effect of water stress and drought on each crop type can be done.

Table 5-3. Kc mean value and the standard deviation of that for initial growth stage

	Cabauw		Loobos		Molenweg		Haastrecht		Oostwaard	
	Kc_mean	Standard deviation	Kc_mean	Standard deviation	Kc_mean	Standard deviation	Kc_mean	Standard deviation	Kc_mean	Standard deviation
2002	0.468558	0.334595	0.437909	0.245595	0.328499	0.261157	0.189359	0.280404	0.348836	0.327703
2003	0.422393	0.323973	0.369309	0.179323	0.189751	0.316995	0.227892	0.279463	0.384968	0.289597
2004	0.517221	0.291435	0.570214	0.225037	0.66619	0.270949	0.563446	0.274732	0.578425	0.283067
2005	0.569548	0.254718	0.536077	0.259855	0.766499	0.258834	0.557319	0.250742	0.604815	0.252612
2006	0.478247	0.313027	0.536014	0.248004	0.403513	0.200072	0.418659	0.286163	0.351571	0.363302
2007	0.632308	0.303088	0.571039	0.258861	0.586378	0.270413	0.447279	0.309732	0.617236	0.291464
2008	0.549966	0.297885	0.385618	0.205623	0.719691	0.268862	0.484004	0.321324	0.544429	0.314247
2009	0.544754	0.308205	0.408937	0.212562	0.696813	0.293199	0.402259	0.370545	0.591809	0.344217
2010	0.518701	0.320568	0.302112	0.165543	0.742314	0.267002	0.553167	0.285054	0.575313	0.295963
2011	0.471519	0.371889	0.514651	0.233712	0.418667	0.241243	0.467467	0.311177	0.499003	0.329051
2012	0.473651	0.242162	0.467015	0.180133	0.459223	0.232778	0.330925	0.214223	0.399199	0.22665

Table 5-4. Kc mean value and the standard deviation of that for initial growth stage

	Vredepeel		Langerak		Dijkgraaf		Zeewolde		Horstermeer	
	Kc_mean	Standard deviation	Kc_mean	Standard deviation	Kc_mean	Standard deviation	Kc_mean	Standard deviation	Kc_mean	Standard deviation
2002			0.323932	0.335719			0.342184	0.361244	0.308188	0.345734
2003	0.356659	0.142353	0.381227	0.330633	0.287993	0.164698	0.484602	0.332572	0.405908	0.31239
2004	0.65786	0.190036	0.584964	0.279131	0.609552	0.258315	0.556624	0.266735	0.571506	0.270116
2005	0.624826	0.25964	0.578059	0.262959	0.592249	0.251127	0.621812	0.224173	0.630943	0.250909
2006	0.621195	0.22312	0.468283	0.317012	0.561584	0.246788	0.540867	0.287957	0.495564	0.297798
2007	0.614968	0.208687	0.576065	0.311054	0.483535	0.231658	0.59449	0.289419	0.61032	0.284949
2008	0.540447	0.188541	0.560463	0.30176	0.320592	0.217027	0.600856	0.265724	0.589077	0.281487
2009	0.621267	0.244532	0.470357	0.387087	0.075341	0.117691	0.525474	0.342139	0.663865	0.244442
2010	0.216094	0.04331	0.601544	0.29082	0.501733	0.222467	0.598425	0.260672	0.590387	0.279839
2011	0.565003	0.267291	0.515685	0.330463	0.499286	0.204723	0.543748	0.316658	0.562423	0.336978
2012	0.58931	0.126482	0.355661	0.225094	0.43204	0.220369	0.475246	0.250199	0.435909	0.248516

Table 5-5. Kc mean value and the standard deviation of that for the mid-season growth stage

	Cabauw		Molenweg		Haastrecht		Oostwaard	
	Kc_mean	Standard deviation	Kc_mean	Standard deviation	Kc_mean	Standard deviation	Kc_mean	Standard deviation
2002	1.034577	0.190346	0.968889	0.057344	0.940228	0.149218	0.893217	0.10354
2003	0.981992	0.111211	1.007593	0.098912	0.956833	0.041713	0.908991	0.032294
2004	0.987543	0.223535	0.891634	0.193995	0.973734	0.076968	0.925047	0.120546
2005	1.017021	0.099948	1.004182	0.07782	0.996781	0.116249	0.946942	0.107634
2006	1.000417	0.150138	1.024508	0.220889	0.9517	0.089529	0.904115	0.07514
2007	1.024195	0.208568	1.006017	0.262495	0.978655	0.122382	0.929722	0.158001
2008	1.08367	0.117546	0.996666	0.084848	0.999232	0.089152	0.94927	0.105984
2009	0.985181	0.130583	0.936558	0.192443	0.968643	0.108045	0.920211	0.127022
2010	0.981019	0.12399	0.942296	0.185251	0.969407	0.109149	0.920937	0.129053
2011	0.975372	0.118243	0.804422	0.243563	0.960418	0.146538	0.912397	0.142143
2012	0.876361	0.282569	0.986458	0.218268	0.960805	0.194247	0.912765	0.16171

Table 5-6. Kc mean value and the standard deviation of that for mid-season growth stage

	Langerak		Zeewolde		Horstermeer	
	Kc_mean	Standard deviation	Kc_mean	Standard deviation	Kc_mean	Standard deviation
2002	1.002833	0.168286	1.042367	0.159725	1.001913	0.135398
2003	1.020339	0.102628	1.063212	0.107418	1.018815	0.16122
2004	1.029813	0.138622	1.002945	0.207533	1.016964	0.181662
2005	1.054075	0.126516	1.077211	0.113633	1.047335	0.123436
2006	1.006414	0.168729	0.987403	0.23621	1.018478	0.153073
2007	1.047757	0.153013	1.015501	0.213756	1.046998	0.156879
2008	1.082497	0.096337	1.048764	0.152783	1.028347	0.148466
2009	1.027356	0.12946	1.005694	0.18427	1.019297	0.145669
2010	1.027551	0.126202	1.00741	0.18058	1.01999	0.145097
2011	1.021384	0.128948	0.989884	0.189407	1.00557	0.168471
2012	1.019333	0.22022	1.018562	0.223541	1.003212	0.235038

If RMSE error of ET estimation for each station compared to heterogeneity result, it shows this heterogeneity affects the value of RMSE.

Doing this monitoring was the end purpose of this research. Because of huge data set and large study area and time limitation this purpose can't be reached, but this result shows the way to reach that and also it shows it is so closed to the last purpose.

6. CONCLUSION AND RECOMMENDATION

In terms of evapotranspiration estimation by SEBS and ground based, fluctuation in the result of ET showed that heterogeneity have impact on ET estimation. So for obtaining more accurate result investigation on heterogeneity is needed. Also weather condition have impact on satellite based data and estimations.

The most important problem in remote sensing work in the Netherlands is the weather condition, because clouds have severe impacts on images. Lack of suitable observation from LANDSAT satellite caused lots of problems in calculating NDVI and deriving high resolution crop coefficient map. As mentioned before for some years there weren't adequate observations for obtaining different steps of crop growth. Although atmospheric correction can decrease this problem, it is a complicated process and takes lots of time, especially in this research that was based on the time series it wasn't possible for this amount of time. Another way can be using also other satellites products that can match. It should be considered working with different satellites will be so complicated because they have different resolution and different calibration. As an example in this research LANDSAT5, LANDSAT 7 and LANDSAT8 images were used. Although they are images from the same group, still matching them with together needed accurate collocation and conversion process.

For investigation of ET heterogeneity, high resolution land cover map is needed. Most of the satellite based land cover maps have coarse spatial resolution, while it doesn't help when the aim is monitoring the impact of drought per each crop type or investigation of ET heterogeneity based on crops variety. The LGN6 land cover maps have a high resolution and it is so useful, but the problem is it is not free.

In terms of crop coefficient, finding crop coefficient value for all types of crops in the study area and for different steps of crop growth, is somehow time consuming, because in FAO_56 it is not available for all of them and needs lots of investigation. With the disaggregated ET products to high resolution water stress ratio can be used for each type of crops that helps to water and food management. As a result availability of high resolution land cover map and information about the land cover characteristics with combination of high resolution suitable satellite images can lead to disaggregation and accurate ET estimation.

LIST OF REFERENCES

2013 World Hunger and Poverty Facts and Statistics by World Hunger Education Service. (n.d.). Retrieved August 25, 2014, from http://www.worldhunger.org/articles/Learn/world hunger facts 2002.htm#Number_of_hungry_people_in_the_world

Abdelrady. (2013). *Evaporation over fresh and saline water using SEBS Evaporation over fresh and saline water using SEBS*.

Allen, R. . (2000). Using the FAO-56 dual crop coefficient method over an irrigated region as part of an evapotranspiration intercomparison study. *Journal of Hydrology*, *229*(1-2), 27–41. doi:10.1016/S0022-1694(99)00194-8

Anderson, M. C., Allen, R. G., Morse, A., & Kustas, W. P. (2012). Use of Landsat thermal imagery in monitoring evapotranspiration and managing water resources. *Remote Sensing of Environment*, *122*, 50–65. doi:10.1016/j.rse.2011.08.025

Anderson, M., & Kustas, W. (2008). Thermal Remote Sensing of Drought and Evapotranspiration. *Eos, Transactions American Geophysical Union*, *89*(26), 233. doi:10.1029/2008EO260001

Baburao Kamble, A. I. and K. H. (2013). Estimating Crop Coefficients Using Remote Sensing-Based Vegetation Index, 1588–1602. doi:10.3390/rs5041588

Bastiaanssen, W. G. M. (2000). SEBAL-based sensible and latent heat fluxes, *229*, 87–100.

Bausch, W. C. (1995). Remote sensing of crop coefficients for improving the irrigation scheduling of corn. *Agricultural Water Management*, *27*(1), 55–68. doi:10.1016/0378-3774(95)01125-3

Beersma, J. J., & Buishand, T. A. (2007). Drought in the Netherlands – Regional frequency analysis versus time series simulation. *Journal of Hydrology*, *347*(3-4), 332–346. doi:10.1016/j.jhydrol.2007.09.042

Broek, J., Teuling, A. J., & Loon, A. F. Van. (2014). COMPARISON OF DROUGHT INDICES FOR THE PROVINCE OF GELDERLAND , THE, (16).

carbo europe. (n.d.). Retrieved from http://gaia.agraria.unitus.it/home

Carter, L., Graham, J., & Notepad, W. (2011). Calculating Vegetation Indices from Landsat 5 TM and Landsat 7 ETM + Data, (January).

Climate Change Effects. (n.d.). Retrieved August 23, 2014, from http://climate.nasa.gov/effects/

Dietz, P. T. J., Put, M. M., & Subbiah, P. S. (n.d.). Drought Risk Assessment for Dryland Agriculture in Semi-arid Telangana, Andhra Pradesh, India. In *Drought Risk Assessment for Dryland Agriculture in Semi-arid Telangana, Andhra Pradesh, India*.

Easterling, D. R., Meehl, G. A., Parmesan, C., Changnon, S. A., Karl, T. R., & Mearns, L. O. (2000). Climate Extremes: Observations, Modeling, and Impacts, *289*(September), 2068–2075.

Eden, U. (2012). DROUGHT ASSESSMENT BY EVAPOTRANSPIRATION MAPPING IN TWENTE, (February).

Edwards. (1997). *CHARACTERISTICS OF 20TH CENTURY DROUGHT IN THE UNITED STATES AT MULTIPLE TIME SCALES*. Colorado State University.

Edwards, D. C., & Mckee, T. B. (n.d.). SPI.

FAO - Food and Agriculture Organization of the United Nations. (n.d.). ETc - Single crop coefficient (Kc). *FAO - Food and Agriculture Organization of the United Nations*. doi:ISBN 92-5-104219-5

Gelassie, T. Y. (2012). REMOTE SENSING EVAPOTRANSPIRATION USING GEONETCAST.

Glenn, E. P., & Brown, P. (2009). Integrating Remote Sensing and Ground Methods to Estimate Evapotranspiration.

Glenn, E. P., Huete, A. R., Nagler, P. L., Hirschboeck, K. K., & Brown, P. (2007). Integrating Remote Sensing and Ground Methods to Estimate Evapotranspiration. *Critical Reviews in Plant Sciences*, *26*(3), 139–168. doi:10.1080/07352680701402503

Gowda, P. H., Colaizzi, P. D., Evett, S. R., Howell, T. A., & Tolk, J. A. (2007). determining exchanges of energy, *50*(5), 1639–1644.

Hayes, M. J., Svoboda, M. D., Wilhite, D. A., & Vanyarkho, O. V. (1999). Monitoring the 1996 Drought Using the Standardized Precipitation Index. *Bulletin of the American Meteorological Society*, *80*(3), 429–438. doi:10.1175/1520-0477(1999)080<0429:MTDUTS>2.0.CO;2

Kalma, J. D., McVicar, T. R., & McCabe, M. F. (2008). Estimating Land Surface Evaporation: A Review of Methods Using Remotely Sensed Surface Temperature Data. *Surveys in Geophysics*, *29*(4-5), 421–469. doi:10.1007/s10712-008-9037-z

Karavitis, C. A., Alexandris, S., Tsesmelis, D. E., & Athanasopoulos, G. (2011). Application of the Standardized Precipitation Index (SPI) in Greece. *Water*, *3*(4), 787–805. doi:10.3390/w3030787

Kite, G. W., & Droogers, P. (2000). Comparing evapotranspiration estimates from satellites , hydrological models and field data, *229*, 3–18.

Kumar, V., & Panu, U. (1997). PREDICTIVE ASSESSMENT OF SEVERITY OF AGRICULTURAL DROUGHTS BASED ON AGRO-CLIMATIC FACTORS ' ture , hydropower generation , water supply , and industries , to name a few . In any such sector in a supply . The determination of these key factors is condition, *33*(6), 1255–1264.

Li, Z.-L., Tang, R., Wan, Z., Bi, Y., Zhou, C., Tang, B., … Zhang, X. (2009). A review of current methodologies for regional evapotranspiration estimation from remotely sensed data. *Sensors (Basel, Switzerland)*, *9*(5), 3801–53. doi:10.3390/s90503801

Liou, Y.-A., & Kar, S. (2014). Evapotranspiration Estimation with Remote Sensing and Various Surface Energy Balance Algorithms—A Review. *Energies*, *7*(5), 2821–2849. doi:10.3390/en7052821

Liu, Y., Xin, X., & Liu, Q. (2009). Modis and Landsat ETM+ scaling study on the daily evapotranspiration over heterogeneous landscapes. In *2009 IEEE International Geoscience and Remote Sensing Symposium* (Vol. 3, pp. III–662–III–665). IEEE. doi:10.1109/IGARSS.2009.5417847

Masek, J., Schwaller, M., & Hall, F. (2006). On the blending of the Landsat and MODIS surface reflectance: predicting daily Landsat surface reflectance. *IEEE Transactions on Geoscience and Remote Sensing*, *44*(8), 2207–2218. doi:10.1109/TGRS.2006.872081

Michael J. Hayes, Mark. D. Svoboda, Donald A. Wilhite, and O. V. V. (1999). Monitoring the 1996 Drought Using the Standardized Precipitation Index, *80*(3). doi:10.1175/1520-0477

Narasimhan, B., & Srinivasan, R. (2005). Development and evaluation of Soil Moisture Deficit Index (SMDI) and Evapotranspiration Deficit Index (ETDI) for agricultural drought monitoring. *Agricultural and Forest Meteorology*, *133*(1-4), 69–88. doi:10.1016/j.agrformet.2005.07.012

Niemeyer, S. (2008). New drought indices, (80), 267–274.

Spiliotopoulos, M., Adaktylou, N., Loukas, A., Michalopoulou, H., Mylopoulos, N., & Toulios, L. (2013). A spatial downscaling procedure of MODIS derived actual evapotranspiration using Landsat images at central Greece. In D. G. Hadjimitsis, K. Themistocleous, S. Michaelides, & G. Papadavid (Eds.), *First International Conference on Remote Sensing and Geoinformation of Environment* (p. 879508). International Society for Optics and Photonics. doi:10.1117/12.2027536

Su, Z. (2002). The Surface Energy Balance System (SEBS) for estimation of turbulent heat fluxes. *Hydrology and Earth System Sciences*, *6*(1), 85–100. doi:10.5194/hess-6-85-2002

Taylor, P., Jiang, L., & Islam, S. (2010). International Journal of Remote Sensing An intercomparison of regional latent heat flux estimation using remote sensing data, (March 2012), 37–41.

Timmermans, J., Su, Z., Pardo, N., Sánchez, M. L., Pérez, I. a., & García, M. A. (2014). SEBS validation in a Spanish rotating crop. *Agricultural and Forest Meteorology*, *195-196*, 132–142. doi:10.1016/j.agrformet.2014.05.007

Timmermans, W. J., Kustas, W. P., Anderson, M. C., & French, A. N. (2007). An intercomparison of the Surface Energy Balance Algorithm for Land (SEBAL) and the Two-Source Energy Balance (TSEB) modeling schemes. *Remote Sensing of Environment*, *108*(4), 369–384. doi:10.1016/j.rse.2006.11.028

Types of Drought. (n.d.). Retrieved August 14, 2014, from http://water.unl.edu/drought/typesofdrought

UNICEF Water and Sanitation. (n.d.). Retrieved August 25, 2014, from http://www.unicef.org/wash/

Vicente-serrano, S. M., Beguería, S., Gimeno, L., Eklundh, L., Giuliani, G., Weston, D., … Pegram, G. G. S. (2012). Challenges for drought mitigation in Africa. *Applied Geography*, *34*, 471–486. doi:10.1016/j.apgeog.2012.02.001

Vicente-Serrano, S. M., Beguería, S., Lorenzo-Lacruz, J., Camarero, J. J., López-Moreno, J. I., Azorin-Molina, C., … Sanchez-Lorenzo, A. (2012). Drought Indices. *Earth Interactions*, *16*(10), 1–27. doi:10.1175/2012EI000434.1

Wright, J. L., Allen, R. G., Tasumi, M., & Trezza, R. (2005). Satellite-Based Energy Balance to Assess Within-Population Variance of Crop Coefficient Curves. *Journal of Irrigation and Drainage Engineering*, *131*(1), 94–109. Retrieved from http://dialnet.unirioja.es/servlet/articulo?codigo=1074090

Yang, F., Zhang, Q., Wang, R., & Zhou, J. (2014). Evapotranspiration measurement and crop coefficient estimation over a spring wheat Farmland ecosystem in the Loess Plateau. *PloS One*, *9*(6), e100031. doi:10.1371/journal.pone.0100031